MONASH University

Development of a process model for the prediction of absorbent degradation during CO_2 capture

Jillian Dickinson

A thesis submitted for the degree of
Doctor of Philosophy at
Monash University
(April 2016)

School of Applied Sciences and Engineering
Faculty of Science

Copyright notice

Declaration

I hereby declare that this thesis contains no material which has been accepted for the award of any other degree or diploma in any university or equivalent institution, and that, to the best of my knowledge and belief, this thesis contains no material previously published or written by another person, except where due reference is made in the text of the thesis.

Name: Jillian Dickinson
Date: 29th April, 2016

Abstract

Fossil fuels are used widely for energy production and are likely to continue to play a major role world wide for many years to come. Much work has been done on the technology for capturing CO_2 from gaseous industrial effluent. For large-scale applications like coal or natural gas-fired power plants, using amine solvents to capture post-combustion CO_2 is the most mature CO_2 capture technology. This technique can be used to retrofit existing plants by treating the flue gas after combustion.

This thesis contains a dynamic mathematical model for the absorber column that can be used to include more detailed reaction chemistry for the absorption of CO_2 into an amine in the presence of O_2 as it becomes available. The dynamic model is constructed from first principles and, while it is built using MEA as the absorbent to remove CO_2, it can be adjusted to cater for the removal of different industrial gases with various absorbents. The model is solved using a commercial solver, MATLAB Ode15s when reduced to a system of ODE's by finite difference in the spatial dimension. The flux of MEA, CO_2, O_2 and H_2O across the phase interface in either direction has been included and more components can be added as required.

The loss of MEA through oxidative degradation has been quantified which is currently not available using commercial packages. Reaction rate kinetics have been employed to predict the accumulation of oxidation products which is limited by the incomplete knowledge of the dominant reactions between O_2 and MEA. When research has produced more detailed information about the products formed during this oxidation, it can be inserted easily into the model.

Validation has been performed using laboratory data from CSIRO Energy Flagship, Newcastle, and data from the CSIRO PCC pilot plant at AGL Loy Yang. A limited parametric study of the impact of operating conditions on oxidation was performed.

Acknowledgements

I have had the privilege of having access to three supervisors, each one of whom is an expert in their field.
I thank Dr Andrew Percy for steering me in the right direction in the process of mathematical modelling, even when I was determined to go in any other direction. His perfectionism both frustrated and confused me but it made me produce the best possible work that I could.
I thank Dr Graeme Puxty for sharing with me his vast knowledge of chemical absorption and how to use the intricacies of the Matlab Suite to their best advantage. Without our impromptu discussions when I got tied up in knots, this work would not have been completed.
I thank Dr T Vincent Verheyen for always checking on me to make sure I was surviving and giving me "verbal CPR" when I wasn't.
Thank you to the people of the Science faculty of the Gippsland campus of the University for their constant support, constructive discussions and encouragement. I also want to thank Dr Eric Meulemann, CSIRO, for giving me the opportunity to do work in this field, Dr Alicia Reynolds and Dr Mai Bui for their support and for always being there when I needed to discuss a problem. To my husband, Ian, for supporting me through the dark nights and for reminding me how much this work meant to me. Without you I would never have reached my goal.
Jillian Dickinson

Contents

Chapter 1

Modelling the CO_2 Capture Process

1.1 Introduction and Background

Fossil fuels are used widely for energy production and, due to their availability and relatively low cost, are likely to continue to play a major role world wide for many years to come [85]. The Intergovernmental Panel on Climate Change report [62] considers the combustion of fossil fuels, such as coal and natural gas, to be the main source of carbon dioxide emissions and that this is the major man-made contribution to global warming. Indicators leading to this conclusion are the relationship between the increase in the global mean temperature and extreme weather conditions, and the acidification of the oceans [84]. Mitigation technologies must be found that stabilise the atmospheric levels of carbon dioxide (CO_2).
Current day ecological problems cannot be solved unless effective clean technologies are developed [73]. Several alternative technologies for capturing CO_2 do exist [34, 85]. Chemical absorption/desorption is currently the most common technology used for CO_2 removal from industrial gases. Treating an acid gas such as CO_2 with alkanolamine solvents is one of the most important commercial technologies because of its technical maturity and extensive use in the refinery industry. This process has been applied to existing coal and natural gas fired power stations in the form of retrofitted plants [15, 58]. It involves the capture of the CO_2 from the flue gas of fossil fuel power plants, followed by the transportation and storage of the liquid CO_2. However, with traditional amine solvents such as monoethanolamine (MEA) or diethanolamine (DEA), a significant energy penalty to the power plant is incurred by the heat and power required to regenerate the amine solvent and compress the CO_2 [16]. Other issues such as solvent degradation and corrosiveness also lead to considerable increases in operating costs. The use of new solvents and

changing process conditions are continually being investigated [17, 66]. With these changes come the involvement of different reactions and more uncertainty as to the emissions from the absorption/desorption system.
In addition to the extensive laboratory work being undertaken, computer simulations are needed to evaluate the new solvents and/or the modified processes. Computer process simulations are recognised as essential tools in chemical process industries and can be used to accurately model these new solvents and processes. Experimental data from operating pilot plants and existing literature has been used for validation. With the simulated program validated, it can be used to assess the feasibility, the economics and the process conditions and to minimise plant pollution. Currently the models do not include the degradation of the solvent over time which effects the efficiency and cost of the process.
There is a need to develop a mathematical model that reflects the true long term dynamic nature of the absorption of CO_2 in MEA, including the evaluation of the extent of degradation of MEA by oxidation in the absorber (and subsequently, by heat in the desorber).
The mathematical model required to describe this process would be a set of differential equations, the solution of which are dependent variables that are expressed as functions of independent variables. The dependent variables include, but are not limited to, the concentrations of the components while the independent variables include, among others, the spatial dimensions of the column and time.
The chemistry of this absorption process is very complicated and in order to develop the model, assumptions have had to be made. The first models, by necessity, ignored all except the basic chemistry and used constants for such variables as density and viscosity which actually change with temperature and concentration. The process reaction chemistry includes reactions between MEA, O_2, CO_2 and H_2O, all of which can have an effect on the efficiency of absorption. The first models only included the major reaction between MEA and CO_2, sometimes the reaction between H_2O and CO_2, but ignored the reaction between MEA and O_2 due to the complexity of the chemistry. The oxidation of MEA is known to have many pathways but the dominating reactions under the absorption conditions are still unknown [88].
These reactions are producing unknown products in the effluents which need to be identified and their influence on the surroundings understood [49, 80]. For over a century, mathematicians have been attempting to produce a mathematical model that will fully describe the process of absorption of carbon dioxide by a solvent. Assumptions have had to be made in order to produce a usable model that resembles reality [11, 19, 57, 61].
Emissions of oxides of carbon, in particular carbon dioxide, occur in large amounts, are generated across the globe and are challenging to address. The absorption

process is being applied to industries whose flue gases contain large quantities of carbon dioxide, such as those burning fossil fuels to produce electricity [5, 71]. Although CO_2 separation using MEA is a relatively mature technology in natural gas sweetening, the process has not been optimized for the abatement of CO_2 emissions in flue gases from fossil fuel fired power plants. The extent of degradation is greater in a flue gas environment. Because of the increased concern with efficiency and the parasitic load on the plant, decreasing the amount of degradation is a much more important issue than in previous applications of the MEA process [78]. Hence the need for the research in this work.

The work of this thesis aims to produce a computer program for the absorption section of the absorption/desorption system which has been coded in such a way that any acid gas and any absorbing solvent, along with the relevant physical and chemical properties, can be inserted into the code as they become known. It can also accommodate different packing elements, and changes in reactive gases and components of the solution. The model can then be used to evaluate the degradation of the solvent and the composition of gaseous emissions from the plant. This provides a means of determining these factors prior to the costly construction of a full scale plant. It can also be utilised to optimise the operating conditions.

Absorption of acid gases is carried out by counter-current contact of a gas stream containing an acid gas (such as CO_2) with an absorbent liquid (often an amine) in a packed column.

$$CO_2 + 2RNH_2 \rightarrow RNHCOO^- + RNH_3^+ \tag{1.1}$$

where R represents an organic or alkoxy molecule associated with the amine group. The "rich" solvent stream leaves the absorber column where the temperature is about 315 K and is fed to a desorber column where the reaction is reversed by the application of heat and the CO_2 is released

$$RNHCOO^- + RNH_3^+ \rightarrow CO_2 + 2RHNH_2 \tag{1.2}$$

The CO_2 is collected as it leaves the desorber column where the temperatures are about 50 K higher and the now "lean" solvent is returned to the top of the absorber column.

Developing an accurate mathematical model to evaluate the mass and heat balances for the absorption and desorption processes has involved adopting some assumptions. The desorption process is complicated by the presence of a condenser at the top and a reboiler at the base of the desorber column. Often flash points exist at the inlet feed of both the vapour (from the reboiler) and the liquid (from the absorber) to the desorber column.

Some mathematical models have assumed that the column is operating in a steady state [58, 77]. There are three types: equilibrium based models, rate based models

and dynamic models. Early equilibrium based models treat the process as if it were at equilibrium throughout the column which is not a true representation of the process of absorption. It was acknowledged that equilibrium is rarely attained since the mass and energy transfer are actually rate processes that are driven by the gradients of chemical potential and temperature [73]. Assumptions were made to cater for the lack of the computational power required to cope with the number of variables that would be otherwise involved and the limited understanding of the chemistry at that time. These equilibrium models simulate the change of concentration and temperature over the height of the column but are not able to be used for prediction of the state of the column after a prolonged period of time [34, 60]. These approaches are usually sufficient to model non-reactive systems but carbon dioxide being absorbed by an MEA solution in the presence of other potentially active components is a reactive system [90]. The equilibrium models were also used to determine the best operating conditions of the CO_2 post-combustion process in order to maximise the CO_2 removal efficiency [57].

In the late 1980's, a rate based model was developed to model continuous, multicomponent operations in an absorber column for the extraction of CO_2 from gases [75]. Whereas previous models had considered the streams fed into the column as either gas or liquid, the rate-based model broke the feed streams into their chemical components. They contained mass and energy conservation equations for the liquid and gas phases, the equations for each phase being connected by mass and energy balances around the interface. Stage temperatures, pressures, vapour and liquid flow rates were taken into consideration but component mole fractions were also important. Boundary conditions needed to be specified for some of the variables in order to have a starting point for the evolution of the numerical solution. Researchers still thought of the liquid and gaseous stream in any particular height increment as being in equilibrium with each other although there was no definitive proof that this was the case.

Several components are present in both the liquid and gaseous phases and all components are involved in a complex series of reactions in the liquid phase [44]. It was assumed that the interface was in thermodynamic equilibrium, that is, properties such as the pressure and temperature at the interface remain unchanged within each height increment. Molar holdup terms, which were ignored in the equilibrium models, were introduced in the component mass balances for the liquid phase in these later models as the processes now had a dynamic nature to them. By considering liquid holdup, an allowance was being made for any liquid that remained on the surface of the packing. The liquid holdup was dependent on the gas and liquid flow rates but the gas holdup was considered negligible due to the low gas density [41, 72].

Resistances to mass and energy transfer in the gas and liquid phases were ac-

counted for by using separate rate equations for each phase which meant that a term for the flux of an individual component from one phase to the other could be incorporated where necessary. Now that the rates of equations were being considered in the process of absorption, the mathematical models had a much wider application. Whereas they were generally used to design the absorption column, they could now also be used to more accurately predict the performance of the column when operating conditions are changed. This would allow for better process control [3].

Dynamic models for the absorption process have been developed and studied but at this stage, they have not been able to include all the complexities of the chemistry involved. The full dynamic nature of the system is unknown and the consequence of reacting CO_2 with MEA in a system containing O_2 is not entirely understood. Dynamic models have been designed that can predict the behaviour response within the column to the changing physical operating conditions such as input gas properties [15, 47]. These models do not assume that equilibrium has been reached at all points and are a closer representation of the real conditions. They include the transfer processes, mass and heat, in order to study the effect of temperature and concentration on the rate of absorption. Limited reaction kinetics are also included as is vapour-liquid equilibrium [19]. The current dynamic models do not include information about the mass transfer of some of the important process components, nor about the degradation of the solvent. Commercial packages such as Aspen Plus and gPROMS do not account for the accumulation of oxidation products. The volatility and the oxidative degradation of the absorbent are long term time-dependent changes that are important to the efficiency of the overall system of absorption.

Several authors investigated the kinetics of the process and concluded that the most important factors to include in the model were the reaction kinetics between carbon dioxide and monoethanolamine (called the carbamate reaction) and the interfacial area [1, 45, 73]. The chemical reactions can be regarded as being instantaneous or kinetically controlled. The dynamic models built in the last fifteen years have been predominately based on six equations and the associated equilibrium constants, reaction rate constants and diffusion rates [35, 48, 71].

Instantaneous equations:

$$\begin{aligned} H_2O &\rightleftharpoons OH^- + H^+ \\ HCO_3^- &\rightleftharpoons CO_3^{2-} + H^+ \\ MEAH^+ &\rightleftharpoons MEA + H^+ \end{aligned}$$

Kinetically controlled equations:

$$\begin{aligned} CO_2 + OH^- &\rightleftharpoons HCO_3^- \\ CO_2 + H_2O &\rightleftharpoons HCO_3^- + H^+ \\ CO_2 + MEA &\rightleftharpoons MEACOO^- + H^+ \end{aligned}$$

Fluxes of CO_2, H_2O and MEA between the gas and the liquid phases are allowed in both directions [19, 32, 45]. However, no consideration is given to any reactions between O_2 and MEA and these are numerous, nor to any reactions involving the other components in the flue gas nor any subsequent reactions involving O_2. This limits the usefulness of the models as predictors of environmental gaseous or liquid discharges or for predicting degradation of the solvent, MEA. While some of these models have assumed that the chemical reactions reach equilibrium, others take a more empirical approach and include an enhancement factor to estimate actual absorption rates from known physical rates [22, 45, 48, 63].
For dynamic simulation and control of complex reactive absorption processes, the model development tries to achieve a balance between the required model accuracy to reflect the process complexity and the feasibility of process simulations regarding the computational time. Descriptions of industrial reactive absorption processes often lead to very extended systems of equations which may not be solved reliably nor quickly enough. Model accuracy increases with complexity but so does difficulty of computation [72].

1.2 Main contribution of the thesis

This thesis contains a dynamic mathematical model for the absorber column that can be used to include more detailed reaction chemistry of the absorption of CO_2 into an amine in the presence of O_2 as it becomes available. It is intended that in the future it will be coupled with models of other sub-processes in order to form a complete model of post-combustion carbon capture using amine systems.

Novelty

- The model can be used to predict absorption chemistry over a long period of time.
- It allows for the flux of any gaseous or liquid component in either direction between the two phases in the absorption column.
- It uses reaction rate kinetics to predict the degradation rate of the amine.

- It predicts the build-up of oxides in the solvent as a result of oxidative degradation of the amine.
- It has been constructed for a column containing random packing and validated with experimental data and data from a retrofitted pilot plant.
- When future, more precise, reaction chemistry becomes known, it can be incorporated into the model.
- It can be modified for absorption of any acid gas into any amine solvent by changing the inputs and the appropriate physical constants.
- CSIRO required a dynamic model that can predict oxidative degradation which the current commercial packages are unable to do at this stage.

1.3 Post-combustion capture of CO_2 with MEA

The absorption/desorption by MEA of the carbon dioxide is a two stage process and consists of separate packed absorption and desorption columns. The process relies on the reversible reaction between carbon dioxide and an amine, most commonly MEA, the direction of the reaction being dependent on the operating temperature. The overall reversible equation can be written as:

$$CO_2 + 2MEA \rightleftharpoons MEACOO^- + MEAH^+ \tag{1.3}$$

At lower temperatures such as are found in the absorber column, reaction (1.3) proceeds to the right and dissolved CO_2 forms a carbamate. When the temperature is increased in the desorber column, the reaction is reversed and the carbamate breaks down into its components, MEA and CO_2, allowing the acid gas to be collected. There is some discussion as to the actual mechanism of the formation of the carbamate [1, 14, 23, 54]. It is thought to occur in two steps [87]

$$CO_2 + MEA \rightleftharpoons MEACOO^- + H^+ \tag{1.4}$$

$$H^+ + MEA \rightleftharpoons MEAH^+ \tag{1.5}$$

with equation (1.4) being slower than equation (1.5) and thus the rate determining step. Within the absorption column, the flue gas, rich in the carbon dioxide, is introduced to the bottom of the column in counter-current contact with an aqueous MEA solution. The packing can be random packing or structured packing, the use of which is required to disturb the flow of the solvent and vapour in order to create a large surface area for mass transfer of components. Gaseous CO_2 is the major component that moves across the gas/liquid interface into the liquid phase. The

CO_2 reacts rapidly in an exothermic reaction with the active solvent component and the carbamate is formed. The gaseous effluent, which is now lean in CO_2, is released into the atmosphere. The solution, rich in the carbamate, continues through the system and is pumped from the bottom of the absorber column to the top of the desorber column. The elevated temperatures in the desorber column cause the reaction to be reversed and the CO_2 is released. The gaseous effluent from the desorber column, consisting of CO_2 and H_2O, is dried and the pure CO_2 is collected for storage or for further use.
The lean MEA solution is removed from the bottom of the desorber, passed through a heat exchanger to reduce its temperature before being returned to a feed tank to ensure a constant feed rate to the absorber. The solvent is made available for further reaction with CO_2. The capacity of an amine to absorb CO_2 by carbamate formation is restricted by stoichiometry to a maximum of 0.5 mole of carbon dioxide per mole of amine. Figure 1.1 is a representation of the absorption/desorption process which details the flow of input vapour and liquid phases but does not show external heat exchangers, condensers, etc.

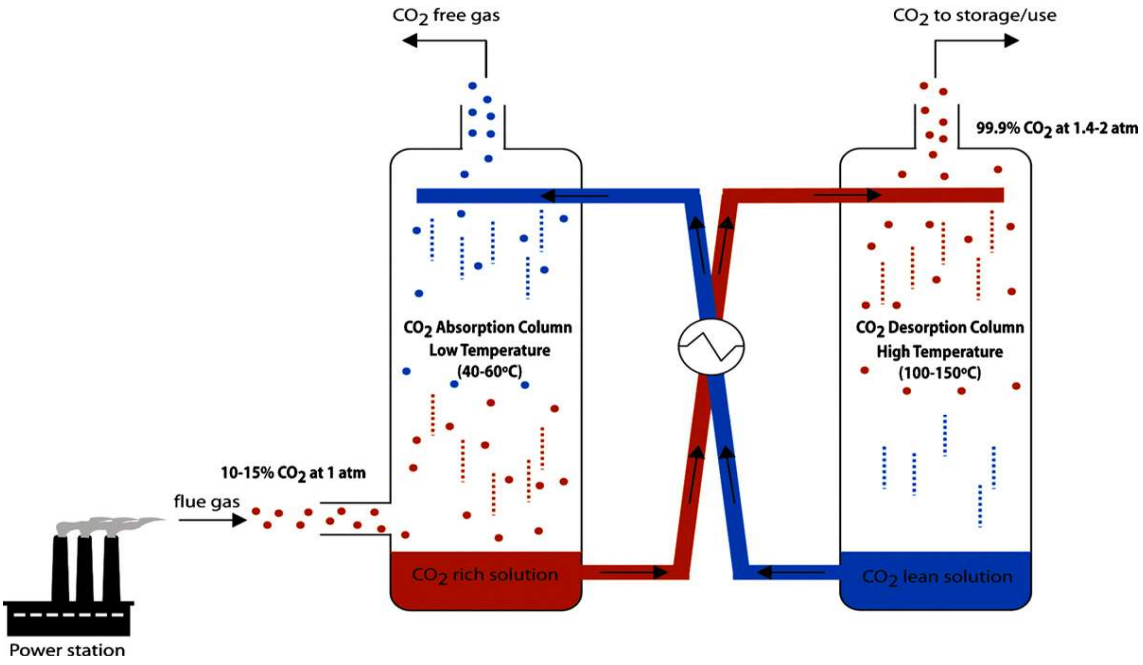

Figure 1.1: Simplified diagram of the absorption-desorption process

1.4 Dynamic modelling of absorption process

CO_2 removal by amine scrubbing has been extensively studied. These studies have focused on optimizing process operating conditions [4, 9, 15], improving or testing new solvents [18, 69], improving the process design to minimize energy consumption [2, 4] and reducing plant efficiency losses [35]. Most of the modeling work on this process has focused on steady state models, that is, they assume that the power plant operates continuously at a given base load. However, power plants are subject to start-up, shut-down and changes in the flue gas load due to fluctuations in the coal feed rate and quality. The operation of the power plant significantly affects the optimum operating conditions of the CO_2 capture process [40]. The last twenty years has seen investigation on variable operations of the power plants using dynamic models [15, 53].

Development of dynamic models is important since there is much information embedded within the dynamics of a plant, which cannot be studied with the steady state models [38]. To be of use the dynamic model of an advanced control application needs to be solved in a fraction of real time. A balance between computational complexity and the accuracy of the prediction is necessary [40]. Many papers discuss the development of dynamic models used to describe the physical and chemical processes that take place in the packed absorption column [9, 19, 35, 41, 45, 48]. Kvamsdal presented a dynamic model of an absorber column in order to study the behaviour of the absorption process downstream of a power plant that operates at varying load but he did not include the vapourisation of MEA [45]. He also used a rate based model but added an enhancement factor that accounted for the reaction kinetics of the model. This method was also used by other modellers [29, 77]. These models assume no volatility of the liquid phase and the main equation considered is that occurring between CO_2 and MEA. The partial differential equations were transformed into ordinary differential equations by discretization of the spatial variable. The mathematical models used a Matlab software package to evaluate the rate of CO_2 absorption changes with respect to the decrease in MEA concentration in the aqueous solution [19]. Greer also discretised the spatial variable and investigated the effect that the physical properties of the absorber, the accuracy of the model and the number of discrete imcrements had on the model computation time [35]. This dynamic model adopted the two-film theory, considered multi-component mass and heat transfer and included some reaction kinetics. It introduced changes to the operating conditions implemented using Matlab in order to observe model efficiency. Greer's model is intended for use for design considerations and also for online control.

Gaspar and Harun developed dynamic models of both the absorber and desorber column and used their models to evaluate the effect of changing the power plant load and of decreasing the temperature of the input rich amine stream [32, 36].

Gaspar validated his model using pilot plant data found in the literature but no degradation chemistry nor loss of MEA were included in their models. Jayarathna worked on a model for the absorber to dynamically predict the plant start up scenario and operation under varying load conditions [40]. Predictions of the transient behavior appear realistic and agree with standard steady state models, but need to be compared with real data as it was validated with literature data only. Kenig developed a dynamic model of reactive absorption using a system of partial differential equations which is solved numerically [41]. The model includes multicomponent two-phase mass transfer, film and bulk reaction mechanisms, fluid dynamic and heat effects. Lawal assumes negligible solvent degradation and shows that the performance of the absorber is more sensitive to the molar ratio between the liquid and gas flow rates, than to the actual flow rates of the liquid solvent and flue gas [47]. This factor has also been demonstrated by Kvamsdal and Zhang [45, 92]. The influence of the temperature and the concentrations of O_2 and CO_2 in the gas feed was studied by Leonard, and their effect on the MEA loss and the emission of degradation products was quantified [49]. This work was all done under controlled conditions in a laboratory. Based on these experimental results, a kinetic relationship for both oxidative and thermal degradation of MEA was proposed. However, these kinetic relationships have yet to be included in a model of a CO_2 pilot plant.

The high energy requirement of the process for solvent regeneration, the loss of the amine solvent by degradation (and consequently the emission of degradation products to the environment) and the corrosive nature of the conditions in the columns represent the main operational negatives associated with the post-combustion CO_2 capture with amines [6, 86]. The degradation and evaporation of MEA results in loss of solvent from the absorption process, which, according to Abu-Zahra [2], requires the replacement of approximately 2.2kg of MEA per tonne of CO_2 captured. Other authors estimate the number of kilograms of MEA lost per tonne of CO_2 to be in the range 0.2 to 3 [33, 42, 59]. Abu-Zahra estimates that the cost of solvent make-up necessary to compensate for this decrease may represent up to 22% of the process operative costs [2]. Oxidative degradation of the MEA is also known to lead to foaming, fouling, increased viscosity of the amine and corrosion of the system [78]. Moreover, the degradation of amine solvents leads to the formation of a large range of by-products that may modify the solvent properties and decrease the process efficiency [49, 70, 78, 81, 88]. Some volatile degradation products like ammonia may then be emitted, potentially resulting in a significant environmental problem with CO_2 capture plants. Although emission reduction technologies exist (such as the (acid) water washing of the flue gas at the column outlet), the problem of volatile products emissions may still be significant in large-scale operating plants [56]. There is no advantage in capturing CO_2 if it implies considerable

emissions of other products such as ammonia and organic acids [82].
Laboratory conditions close to those of an industrial absorption plant were adopted by Lepaumier [50] and in a separate work by Leonard [49], but no kinetic model of solvent degradation was proposed. Both papers indicate that MEA oxidative degradation is the main cause of degradation in industrial conditions but the actual products being emitted from the absorber column are not specified. Although previous studies have led to a better understanding of the solvent degradation mechanisms, there is currently no validated kinetic model of MEA degradation that is able to predict industrial scale degradation. Based on experimental results, Leonard proposes a kinetic relationship for solvent degradation. It was found that the oxidative degradation of MEA does not depend on the CO_2 concentration when CO_2 is present in the gas feed, and that a higher degradation rate is observed when no CO_2 is present. The CO_2 loading appears to inhibit MEA oxidative degradation [49, 81]. These results also confirm that the main degradation pathway is the oxidation reaction since no MEA loss can be observed in the absence of oxygen [49].

1.5 Oxidation of MEA

Amines have been used for decades for the removal of CO_2 from hydrocarbon streams [43] but their use in an oxidising environment such as is found in a brown coal fired power station flue gas is limited [7]. Oxidation of MEA is slow at room temperature but occurs readily at high temperatures. The conditions in the absorber column are higher than room temperature but still low relative to pyrolysis [7].
In an ideal MEA-CO_2 absorption system, the solvent is cycled through the absorber/desorber system. Some of the byproducts of MEA oxidative degradation can decrease the efficiency of CO_2 capture and have also been implicated in the corrosion of machinery and toxicity to the environment [8, 68]. There has been an awareness for over fifty years that the oxidative degradation of MEA needs to be considered when constructing a model of CO_2 absorption by MEA, but it has been a very difficult task to undertake [64, 70]. Much research has been done on the reactions that may occur between O_2 and MEA and several authors are in some agreement as to what these reactions and products are [76, 80, 88, 89]. Formic, oxalic and glycolic acids are the main carboxylic acids identified in degraded MEA samples from industrial pilot plants and their formation was reported in many experimental studies [33, 49, 59]. Other products include, but are not limited to, ammonia, 1-(2-hydroxyethyl)-formamide, 1-(2-hydroxyethyl)-imidazole, acetamide, and oxalamide. Vevelstad [88] states there are nineteen reactions that could take place within the conditions that would be found in the

absorber column. Some authors have listed possible formation pathways of degradation products from the oxidation of primary amines [51].
The development of a dynamic model without including the specific reaction(s) for the oxidation of MEA is complex. Several papers have explained experimental work that was done in order to determine an overall reaction rate for the oxidation of MEA that can be used when incorporating the oxidative degradation of MEA into a model for the CO_2 absorber column [49, 81, 86]. Uyanga developed two kinetic models to predict the MEA degradation rate in the presence of SO_2 and O_2. The first can be used when MEA, CO_2, O_2 and SO_2 are present in the model. The second is a more general model and allows for the SO_2 and/or O_2 concentration to be positive or zero [86]. Supap did more experimentation and developed a rate equation that can be used with any of CO_2, O_2 and SO_2 removed without affecting the usability of the model [81]. Leonard found that the presence of CO_2 created an inhibiting effect on the oxidative degradation of MEA and this effect does not depend on the concentration of the CO_2. The influence of CO_2 can be neglected as it is always present in the capture process [49]. Since MEA is always present in large excess in the absorber column under discussion and thus is not a limiting factor, its influence on the degradation kinetics can also be ignored. Based on the fact that the concentration of MEA and CO_2 does not influence the degradation in the absorber, Leonard has described a relationship for the reaction rate for MEA oxidative degradation. This reaction rate formula has been used in this work and even though the precise chemical reaction (or reactions) are unknown, the amount of MEA oxidation products building up in the absorber over time can be predicted using this relationship.

1.6 Chemistry

The chemistry of this carbon capture process is complex and difficult to fully model. Prior to entry into the absorber column the industrial effluent gas has had the solid particulates and the various sulphates and nitrates removed in order to reduce their impacts on the absorption process. When it enters the absorber column, the flue gas is mainly CO_2, O_2, H_2O and N_2. The MEA solvent, which is recirculated into the top of the absorption column, initially contains MEA and H_2O. During the vertical movement of the phases through the column the components transfer between the two phases. CO_2 and O_2 diffuse from the gaseous phase to the liquid phase due to the concentration differential. A small amount of MEA is vapourised from the liquid phase into the gaseous phase and is then exhausted from the absorber column. The effluent gas is moist, and the liquid solvent is approximately seventy per cent water, so the H_2O can move either way between the phases. The temperature and pressure at the position in the column

dictates which way the flux occurs. As well as the transfer of components between phases, there are also changes in concentration of the components of each phase as they move the length of the column due reactions occurring in the liquid phase. As the liquid phase flows down the length of the column, the CO_2 is transferred into it and then reacts with the MEA to form the carbamate. The concentration of MEA decreases whilst the concentration of the carbamate increases. The CO_2 can also react with the H_2O in the liquid phase but the reaction is very slow compared to the reaction between CO_2 and MEA [34, 74]. The former reaction can be considered inconsequential in concentrated amine solutions such as those found in the absorber system. O_2 also oxidises the MEA when it enters the liquid [88]. This is discussed in detail in Section 2.2.3.
There are several influences on the internal temperature of the two phases in the absorber column although the column itself is assumed to be adiabatic. The temperature differential between the two phases results in the transfer of heat from one phase to the other. The reactions occurring in the liquid phase are exothermic. The vapourisation of MEA causes a decrease in the temperature of the liquid and increases that of the gas, whilst the movement of water either increases or decreases the energy content of the phases depending on whether it is condensing or vapourising.

1.7 Deficiencies of Current Absorption Models

Previous models do not include all the chemical changes discussed in section 1.6 due to the difficulty in modelling them and also to the lack of chemical data for some of the processes. For example

- Flux of O_2 from gas to liquid has not been considered
- Predominant reaction chemistry between MEA and O_2 is not known.
- Reaction between MEA and O_2 not included - therefore there is no knowledge of the amount of MEA involved in any irreversible reactions and thus withdrawn from the absorption process.
- Few models include vapourisation of MEA [71]
- Build up of oxidation products has been ignored.
- Emissions to the atmosphere of products containing nitrogen are unknown over the long term

These points mean that the amount of MEA that is no longer available for reaction with CO_2 as the solvent cycles throughout the absorber/desorber system is not

accounted for. This should not be ignored as the efficiency of the column is effected by the withdrawal of available MEA and there are risks in atmospheric emissions of unknown nitrogen containing degradation products. The model proposed in this thesis includes the flux of O_2, CO_2, H_2O and MEA. This allows for the inclusion of the vapourisation of MEA which is subsequently lost to the absorption process and oxidative degradation of MEA which results in the build-up of oxidation products in the liquid phase. The decrease of MEA by these two actions affects the efficiency of the absorption system and hence the cost.

Chapter 2

Development of the Model

2.1 Building the model

Absorption of a gas into a liquid involves flux across the gas/liquid interface, followed by reaction in the liquid phase. The energy levels change as a result of chemical reactions in the liquid, the heat of absorption of gaseous components in the liquid and the heat of evaporation of liquids to the gaseous phase. The absorption scenario can be described using an advection-reaction equation [30] where the evolution of the chemical components can be derived from changes in the mass balances. As the flow in an absorption column is counter-current and the two phases have differing initial temperatures, the temperature throughout the height of the column is also changing. This varying temperature affects the rates of reaction, the rate of flux and other physical properties of the liquid and the gas, such as density and viscosity. In order to increase the surface area between the two phases to allow for greater mass transfer, the absorption column contains random packing which influences the fluid dynamics. Consideration needs to be given to the properties of the packing, such as liquid and gas holdup.
Unlike many previous models which consider absorption of CO_2 into an aqueous solution of MEA as a system of five components [26, 31], this model is a system of seven components which can be expanded to include other components as required. They include

- an inert carrier gas, N_2,
- two reactive gaseous, O_2 and CO_2,
- two volatile components of the solution, H_2O and MEA,
- a non-volatile carbamate that is decomposed by heat, and
- non-volatile soluble products that are oxides of MEA.

Currently, the precise proportions of products resulting from the oxidation of MEA under absorber conditions are unknown and this model has been written so that any future chemistry can be encoded as it becomes identified. As the oxidation products of MEA are known to be soluble heat stable salts and the heat in the stripper does not effect them, they build up in the liquid solvent as they recirculate through the absorber-desorber system. The accumulation of these oxidation products is very slow but needs to be quantified, so the time that the system is run for validation becomes important.
The proposed model is a dynamic model of the absorber system which considers the chemistry of the changing absorption system. It includes the decrease of available MEA for absorption and the build up of oxidation products. This dynamic mathematical process model is a system of partial differential equations(PDE's) with independent variables column height and time. The PDE's have been developed from advection, flux and reaction equations which have been applied to the absorption column. The system is used to describe the effects of operational changes on the column but more importantly, the real time degradation of MEA with oxygen.
The model contains a differential equation for each of the components of interest in the liquid and gaseous phases and for the temperature of each phase. The components included in the model are MEA, H_2O, $MEACOO^-$, $MEAH^+$, CO_2 and O_2 in the liquid phase and H_2O, CO_2, MEA and O_2 (present as a component of air) in the gaseous phase. The N_2 in the air is not regarded as being involved in the mass transfer nor in any reactions. In the liquid phase there is also a general term for the oxidation products, OP, that occur as a result of reaction between MEA and O_2. The physical properties of the system such as density, viscosity and specific heat capacity are expressed in terms of concentration and temperature and thus vary depending on the conditions at the relative position in the column and over time.
As with other dynamic models, this model contains the following assumptions.

- Both liquid and vapour phases are ideal mixtures.
- Liquid and vapour velocities within the absorber column are assumed to be constant.
- Vertical diffusion within each phase is regarded as negligible when compared to the advection/reaction effects.
- The absorption column is operated adiabatically.
- Interfacial surface area is the same for heat and mass transfer.
- Chemical reactions take place in the liquid phase only.

- Due to a small liquid phase heat transfer resistance, the liquid interface temperature can be considered equal to the bulk liquid temperature.

Mass balance equations determine the change of concentrations with time and column height and the enthalpy balance determines the change in temperature with time and height. The equation for the mass balance in the liquid phase, equation (2.1), states that the change of concentration of a component, i, in the liquid, C_{li}, with time, t, is equivalent to the advection of the component in the liquid flow plus the diffusion of i into or out of the liquid phase plus the rate of generation or consumption of i due to reaction. The equation for the vapour, equation (2.2), is similar but there is no reaction term. Component mass balance for the liquid phase is:

$$\frac{\partial C_{li}}{\partial t} = u_l \frac{\partial C_{li}}{\partial z} + \frac{a_{wl} N_i}{L} + \frac{R x_i}{L} \tag{2.1}$$

and for the gas phase is:

$$\frac{\partial C_{gi}}{\partial t} = u_g \frac{\partial C_{gi}}{\partial z} - \frac{a_{wg} N_i}{G} \tag{2.2}$$

where subscripts li and gi represent the liquid and gas phase components respectively, t is time (sec) and z is the height of the packing (mol). L and G are functions of z and t and are the total moles of the liquid and gas(mol m^{-3}), N_i is the molar flux between the phases (mol m^{-2} s^{-1}) and a_{wl} and a_{wg} is the effective interfacial area of packing per unit volume of liquid and gas (m^2 m^{-3}), see Section 2.2.2. R_{xi} is the consumption or production of component i as a result of any reaction. u_l and u_g are the liquid and gas velocities (m s^{-1}) with the direction of the gas flow regarded as being positive and that of the liquid flow negative.
As the concentration of the liquid and the gas are measured in mole m^{-3} and thus their compositions change constantly due mainly to flux and reactions, an equation for this change is required for L and G. They change with respect to z and t according to

$$\frac{\partial L}{\partial t} = u_l \frac{\partial L}{\partial z} + a_{wl} \sum N_i + \sum R x_i \tag{2.3}$$

$$\frac{\partial G}{\partial t} = u_g \frac{\partial G}{\partial z} - a_{wg} \sum N_i \tag{2.4}$$

The equation for the change of liquid temperature with time and height, equation (2.5), is the advection of heat content of the liquid plus the flow of heat between phases due to the temperature gradient, plus the heat released or absorbed when the components condense or evaporate, plus the heat released or consumed by any

reactions, as well as a term for the change in temperature due to the transfer of components from one phase to the other. Heat balance for the liquid phase is:

$$\frac{\partial T_l}{\partial t} = u_l \frac{\partial T_l}{\partial z} + \frac{h_T a_{wl}(T_l - T_g)}{LC_{pl}} + \frac{a_{wl} \sum N_i \Delta H_{vap}}{LC_{pl}} + \frac{\Delta H_{Rx}}{LC_{pl}} + \frac{a_{wl}(T_l - T_g) \sum N_i C_{pi}}{Lc_{pl}} \tag{2.5}$$

where h_T is the heat transfer coefficient (W m^2 K), ΔH_{vap} and ΔH_{Rx} are the heat of vapourisation and reaction respectively (J mol^{-1}) and C_{pl} is the specific heat capacity of the liquid (J mol^{-1} K^{-1}). T is the temperature in Kelvin and and a_w is the interfacial area of packing per volume of packing in the column (m^2 m^{-3}). The gas phase heat balance, equation (2.6), consists of the advection term plus the heat flow due to the temperature gradient between the phases and a term for the change in temperature due to the transfer of components from one phase to the other. Heat balance for the gas phase is:

$$\frac{\partial T_g}{\partial t} = u_g \frac{\partial T_g}{\partial z} + \frac{h_T a_{wg}(T_g - T_l)}{GC_{pg}} + \frac{a_{wg}(T_g - T_l) \sum N_i C_{pi}}{GC_{pg}} \tag{2.6}$$

where C_{pg} is the specific heat capacity of the gas (J mol^{-1} K^{-1}). For ease in computation the model is developed using mole fraction as the unit of quantity.

2.2 Mass Transfer

The mass balance equation for the liquid phase, (2.1), and for the vapour phase, (2.2), can be constructed as follows.

2.2.1 Advection

Advection is the vertical movement of the components within the liquid and vapour phases and is due to the bulk motion of the liquid and vapour [37]. It is represented by the advection equation.

$$\frac{\partial C_i}{\partial t} = -u\frac{\partial C_i}{\partial z} \tag{2.7}$$

C_i concentration of component mole fraction

Interfacial area and mass transfer parameters are dependent on column dimensions, operating conditions, (e.g. input flow rates, liquid properties including liquid hold-up and diffusion coefficients) and packing constants. The different types of packing have associated specific constants that represent the construction of the packing, the dimension and the specific surface area of the packing. These characteristics have an impact on the hydraulic properties of the absorption column.

2.2.2 Flux

Flux is defined as the flow of a component from one phase to the other phase.

$$\text{Flux term} = \frac{N_i\ a_{wl}}{L} \tag{2.8}$$

There is a similar equation for gas. In this model, the transfer of mass and energy from the gas to the liquid is considered as positive. The flux term accounts for the amount of the component that crosses the phase interface at a given instant and height.

1. **Flux through interfacial area**

   The molar flux of a component i that crosses the vapour-liquid interface is described by the overall mass transfer expression [22]

   $$N_i = K_{gi}(P_i - P_i^*) \tag{2.9}$$

K_{gi}	overall mass transfer coefficient	moles Pa^{-1} m^{-2} s^{-1}
P_i	vapour pressure in the bulk vapour	Pa
P_i^*	equilibrium partial pressure in the bulk liquid	Pa

$(P_i - P_i^*)$ is the pressure differential and the driving force for the flux. If $(P_i - P_i^*)$ is positive, the component moves from the vapour to the liquid, if negative, the component moves from the liquid to the vapour.

2. **Overall Mass Transfer**

The mass transfer coefficients for both liquid and vapour are sourced from Billet and Schultes [10]. Using the two film theory, the overall mass transfer coefficient for the vapour components incorporating liquid and vapour side transfer resistance is

$$\frac{1}{K_{gi}} = \frac{1}{k_{gi}} + \frac{H_i}{E k_{li}} \tag{2.10}$$

H	Henry's constant	Pa m^3 mol^{-1}
i	CO_2, O_2, and H_2O	
k_{gi}	mass transfer coefficient of i in the vapour phase	mol Pa^{-1} m^{-2} s^{-1}
k_{li}	mass transfer coefficient of i in the liquid phase	m s^{-1}
E	enhancement factor due to chemical reaction	

Henry's constant is calculated in point 8 below.

3. **CO_2 Enhancement Factor**

Mass transfer is increased by chemical reaction. The enhancement factor compares the level of mass transfer when reaction occurs to that when there is no reaction and is represented by the following equations [22].

$$M = \frac{D_{lCO_2} r}{(k_{lCO_2})^2}$$

$$E = \sqrt{M} \coth(\sqrt{M})$$

D_{lCO_2}	liquid phase diffusion coefficient of CO_2	m^2 s^{-1}
r	reaction rate	s^{-1}

The definition for the diffusion coefficient of a solute in a solvent is taken from Cussler [22].

$$D_{lCO_2} = \frac{7.4 \times 10^{-8} (\phi MW_{H_2O})^{0.5} T_l}{\nu_{H_2O} {V_{CO_2}}^{0.6}} 10^{-4} \tag{2.11}$$

ϕ	empirical parameter for water	
MW	molecular weight	
ν_{H_2O}	viscosity of water	cP
V	molar volume at normal boiling temperature	$cm^3\ mol^{-1}$

$$\nu_{H_2O} = e^{\left(\frac{897.9879}{{T_C}^{0.6542}+78.1912}\right)} - \frac{17.6724}{{T_C}^{0.004707}} \tag{2.12}$$

T_C temperature Celsius

Gaseous diffusion coefficient was also adopted from Cussler.

$$D_{gCO_2} = \frac{1.8610^{-3}T^{1.5}(\frac{1}{MW_{CO_2}} + \frac{1}{MW_{N_2}})^{0.5}}{P{\sigma_{CO_2,N_2}}^2\Omega_{CO_2,N_2}} \tag{2.13}$$

σ	collision diameter	Angstroms (Parameter from Poling)
Ω	Lennard-Jones potential	dimensionless (Parameter from Poling)

4. CO_2 mass transfer

The mass transfer of CO_2 occurs in both phases. The molar flux of CO_2 across the vapour/liquid interface is driven by

$$N_{CO_2} = K_{gCO_2}(P_{CO_2} - P^*_{CO_2}) \tag{2.14}$$

The overall mass transfer coefficient K_{gCO_2} is as described in equation (2.10) and includes the mass transfer coefficients in both the gas phase and the liquid phase. The mass transfer coefficient for CO_2 in the gas phase k_{gCO_2} is [10]

$$k_{gCO_2} = c_v \frac{1}{(\epsilon - h_l)^{1/2}} \frac{a^{3/2}}{d_h^{1/2}} \frac{D_{gCO_2}}{a} \left(\frac{u_g}{(a\nu_{kg})}\right)^{3/4} \left(\frac{\nu_{kg}}{D_{gCO_2}}\right)^{1/3} \tag{2.15}$$

c_v	packing specific constant	
ϵ	packing void fraction constant	$m^3\ m^{-3}$
a	specific surface area of dumped packing	$m^2\ m^3$
h_l	liquid holdup	$m^3\ m^{-3}$
D_{gCO_2}	Diffusion coefficient in the gas	$m^2\ s^{-1}$
ν_{kg}	kinematic gas viscosity	$kg\ m^{-3}$

The mass transfer coefficient for CO_2 in the liquid phase is expressed as [10]:

$$k_{lCO_2} = c_l 12^{1/6} \left(\frac{u_L}{h_L}\right)^{1/2} \left(\frac{D_{lCO_2}}{d_h}\right)^{1/2} \tag{2.16}$$

u_L	velocity of liquid with respect to empty column cross-section	mol s^{-1}
c_l	packing specific constant	
d_h	hydraulic diameter of the random packing	m

The liquid hold-up is defined as the volume of liquid forming a film on the surface of the packing or drops in the void space of the packing [79].

$$h_l = (\frac{12 u_l a^2 \nu_{dl}}{g \rho_L})^{1/3} \tag{2.17}$$

ν_{dl}	dynamic liquid viscosity	kg m^{-1} s^{-1}
g	gravitational constant	m sec^{-2}
ρ_L	density of the liquid	kg m^{-3}

Dynamic (or shear) liquid viscosity ν_{dl} is defined [91] as

$$\nu_{dl} = \nu_{H_2O} e^{(\frac{100(t_2)(t_3+1)C_{MEAl}}{T_l{}^2})} \tag{2.18}$$

where

$$t_2 = 21.186 cMEA_l + 2373 \tag{2.19}$$

$$t_3 = \frac{C_{CO_2 l}}{C_{MEAl}}(0.01015 C_{MEAl} 100 + 0.0093 T_l - 2.2589) \tag{2.20}$$

$cMEA_l$	mass fraction of MEA
C_{MEAl}	mole fraction of MEA
$C_{CO_2 l}$	mole fraction of CO_2

Kinematic liquid viscosity ν_{kl} is [91]

$$\nu_{kl} = \frac{\nu_{dl}}{\rho_L} \tag{2.21}$$

The density of the gas is defined as the density of the individual gases multiplied by the mole fraction of each component gas [71].

$$\rho_G = \sum \rho_{gi} C_i \tag{2.22}$$

where i are the components of the gas.

The density of the liquid is more dependent on the liquid temperature and concentration.

$$\rho_{L_{20}} = (-0.000515847 T_c + 0.15402 \frac{[CO_2]}{[MEA]} + 1.016)1000 \tag{2.23}$$

$$\rho_{L_{30}} = (-0.000541818T_c + 0.23345\frac{[CO_2]}{[MEA]} + 1.016)1000 \tag{2.24}$$

$$\rho_{L_{40}} = (-0.000541091T_c + 0.31642\frac{[CO_2]}{[MEA]} + 1.015)1000 \tag{2.25}$$

$\rho_{L_{20}}$	density of liquid at 20^o C	mol m^{-3}
$\rho_{L_{30}}$	density of liquid at 30^o C	mol m^{-3}
$\rho_{L_{40}}$	density of liquid at 40^o C	mol m^{-3}
T_c	critical temperature	K
$[CO_2]$	concentration of CO_2	mol m^{-3}
$[MEA]$	concentration of MEA	mol m^{-3}

If $[MEA] \leq 0.20$, then the density of the liquid is $\rho_{L_{20}}$.
If $0.20 < [MEA] < 0.30$, then the density of the liquid is calculated from

$$\rho_L = (X \times \rho_{L_{20}}) + ((1 - X) \times \rho_{L_{30}}) \tag{2.26}$$

where

$$X = (0.3 - [MEA])10 \tag{2.27}$$

If $[MEA] \leq 0.30$, then the density of the liquid is $\rho_{L_{30}}$.
If $0.30 < [MEA] < 0.40$, then the density of the liquid is calculated from

$$\rho_L = (X \times \rho_{L_{30}}) + ((1 - X) \times \rho_{L_{40}}) \tag{2.28}$$

where

$$X = (0.4 - [MEA])10 \tag{2.29}$$

If $[MEA] == 0.40$, then the density of the liquid is $\rho_{L_{40}}$.

5. **O_2 mass transfer**

O_2 has low solubility in liquids thus the Henry's Law constant for O_2 is very large. This results in the mass transfer being slowest in the liquid and thus the controlling factor. The overall mass transfer coefficient, equation (2.10) can be reduced to

$$K_{gO_2} = \frac{k_{lO_2}}{H_{O_2}} \tag{2.30}$$

where k_{lO_2} is the mass transfer coefficient of O_2 in the liquid. No enhancement factor is necessary as the reaction occurs very slowly and any resulting mass change is also very slow.

6. **H_2O mass transfer**

As the liquid is mainly water and MEA, it can be assumed that there is negligible liquid resistance to the mass transfer of water and the term $\frac{H_{CO_2}}{Ek_{lCO_2}}$ in (2.10) is assumed to be 0. The overall mass transfer coefficient for water can be regarded as equivalent to the mass transfer of the water in the gaseous phase.

$$K_{gH_2O} = k_{gH_2O} \tag{2.31}$$

where k_{gH_2O} is equivalent to equation (2.15).

7. **MEA mass transfer**

It can also be assumed that there is negligible liquid resistance to the mass transfer of MEA and thus the overall mass transfer coefficient for MEA is

$$K_{gMEA} = k_{gMEA} \tag{2.32}$$

where k_{gMEA} is equivalent to equation (2.15).

8. **Equilibrium Partial Pressure**

The equilibrium partial pressure of CO_2 and O_2 in the bulk liquid is expressed by Henry's Law which is a measure of the solubility of the gas in the given liquid. Henry's Law (for gases) for a binary system need not assume an ideal gas phase [65].

$$P_i^* = H_i C_i \tag{2.33}$$

i CO_2 or O_2

Henry's Law for CO_2 in water, H_{CO_2} (in Pa) [21] is

$$H_{CO_2} = 10^5 e^{(4.8 + \frac{3934.4}{T_l} - \frac{941290.2}{{T_l}^2})} \tag{2.34}$$

where T_l is the temperature of the liquid and is $\leq 353K$.

Henry's Law for O_2 in water, H_{O_2} (in Pa) [67] is

$$H_{O_2} = 10^5 \frac{P_{O_2}}{mO_2} \tag{2.35}$$

P_{O_2} partial pressure of oxygen Pa
mO_2 mole fraction of oxygen

Henry's Law for CO_2 and O_2 are also used in the calculation of the mass transfer coefficients in point 2 of this section.
Raoult's law is used to model ideal liquids.
The equilibrium partial pressure of H_2O and MEA in the bulk liquid is calculated using Raoult's Law.

$$P_i^* = P_{vpi} C_i \tag{2.36}$$

i H_2O or MEA,
P_{vp} the partial vapour pressure of the component Pa

According to Raoult's Law [55, 65]

$$P_{vpH_2O} = 10^5 \times 10^{(5.11564 - \frac{1687.537}{T_l + 230.17 - 273.15})} \tag{2.37}$$

$$P_{vpMEA} = 92.624 - \frac{10367}{T_l} - 9.4699 \log_e T_l + 1.9 \times 10^{-18} {T_l}^6 \tag{2.38}$$

9. **Wetted surface area**

The wetted surface area available in the column, a_w, is the surface area of packing per volume of packing [10].

$$a_w = 1.5(a\ d_h)^{-0.5} \left(\frac{u_l\ d_h}{(\nu_{kl})^{-0.2}} \right) \left(\frac{(u_l)^2\ \rho_L\ d_h}{(\sigma_l)^{0.75}} \right) \left(\frac{(u_l)^2}{(g\ d_h)^{-0.45}} \right) a \tag{2.39}$$

$$d_h = 4 \frac{\epsilon}{a} \tag{2.40}$$

σ_l surface tension of the liquid phase kg m^{-2}
ν_{kl} kinematic liquid viscosity kg m^{-3}

By definition, the kinetic liquid viscosity is equal to the dynamic liquid viscosity divided by the density of the liquid [65].

$$\nu_{kl} = \frac{\nu_{dl}}{\rho_L} \tag{2.41}$$

For equations (2.1) - (2.6), a_w needs to be in the form of area of packing per volume of liquid, or gas, rather than area of packing per volume of packing, and has been denoted a_{wl} and a_{wg}.

$$a_{wl} = \frac{a_w}{h_l} \tag{2.42}$$

$$a_{wg} = \frac{a_w}{h_g} \tag{2.43}$$

The liquid holdup, h_l (m^3 m^{-3}), is the volume of the packed column that is occupied by the liquid at a given time (Equation (2.17)) whereas the remaining void space in the column is assumed to be occupied by the gas [10]. The gas hold-up is defined as the volume of the packed column less the volume of the packing and the volume of the liquid in the column.

$$h_g = \epsilon - h_l \tag{2.44}$$

h_g gas hold-up m^3 m^{-3}

2.2.3 Reaction

The reaction term caters for the change of concentration resulting from any reactions that take place in the liquid. It represents the number of moles of the component that are created or consumed per second due to reaction expressed as a mole fraction.

$$\text{reaction term} = \frac{Rx_i}{L} \tag{2.45}$$

where Rx_i has units mole m^{-3} s^{-1}.
Two reactions are included in this model. The main absorption reaction represents the removal of carbon dioxide from the vapour effluent when it reacts with MEA in the liquid phase at low temperatures. It is a rapid two stage reaction:

$$CO_2 + MEA \rightleftharpoons MEACOOH \tag{2.46}$$

The forward reaction rate, k_f, for equation (2.46) is

$$k_f = \frac{[MEACOOH]}{[CO_2][MEA]} \tag{2.47}$$

and the reverse reaction rate, k_r, is

$$k_r = \frac{[CO_2][MEA]}{[MEACOOH]} \tag{2.48}$$

The change of concentration of CO_2, Rx_{CO_2}, for equation (2.46) is

$$Rx_{CO_2} = -k_f[CO_2][MEA] + k_r[MEACOOH] \tag{2.49}$$

$$MEACOO^- + H^+ \rightleftharpoons MEACOOH \tag{2.50}$$

The equilibrium constant, $K2$, for equation (2.51) is

$$K2 = \frac{[MEACOOH]}{[MEACOO^-][H^+]} \tag{2.51}$$

$$MEA + H^+ \rightleftharpoons MEAH^+ \tag{2.52}$$

The equilibrium constant, $K3$, for equation (2.53) is

$$K3 = \frac{[MEAH^+]}{[MEA][H^+]} \tag{2.53}$$

The overall equation, which has been included in all previous modelling of CO_2 and MEA is

$$CO_2 + 2MEA \rightleftharpoons MEACOO^- + MEAH^+ \tag{2.54}$$

The forward reaction rate for equation (2.54) is k_f^1 and the reverse reaction rate is k_r^1. Rx_{CO_2}, for equation (2.54) is

$$Rx_{CO_2} = -k_f^1[CO_2][MEA]^2 + k_r^1[MEACOO^-][MEAH^+] \tag{2.55}$$

Equating equation (2.49) with equation (2.55):

$$k_f^1 = \frac{k_f}{[MEA]} \tag{2.56}$$

and

$$k_r^1 = \frac{k_r[MEACOOH]}{[MEACOO^-][MEAH^-]} \tag{2.57}$$

From equation (2.51) and equation (2.53)

$$\frac{[MEACOOH]}{[MEACOO^-][MEAH^+]} = \frac{K2}{K3[MEA]} \tag{2.58}$$

Thus equation (2.55) can be written

$$Rx_{CO_2} = -k_f[CO_2][MEA] + \frac{k_r K2[MEACOO^-][MEAH^+]}{K3[MEA]} \tag{2.59}$$

This is the overall reaction rate, r, for equation ((2.54)) where r equals Rx_{CO_2}.

The reaction of concern in this work is that between oxygen and MEA which is irreversible and thus withdraws some of the MEA from the absorption system.

$$XO_2 + YMEA \longrightarrow \text{oxidation products} \tag{2.60}$$

where X and Y represent the unknown amounts of oxygen and MEA (respectively) involved in any reaction. Due to the many possible reactions between these two compounds, it is difficult to choose one reaction that is more important than the others for oxidative degradation [8]. Some of the reactions that have been identified as producing formic, oxalic and glycolic acids are as follows:

$$MEA + \frac{1}{2}O_2 \longrightarrow HCOOH + CNH_2 \tag{2.61}$$

$$MEA + 2O_2 \longrightarrow HOOCCOOH + NH_3 + H_2O \tag{2.62}$$

$$MEA + O_2 \longrightarrow HOCH_2COOH + NH_3 \tag{2.63}$$

It has been noted by Vevelstad that there are nineteen reactions that could take place between oxygen and MEA depending on the conditions within the column [88]. Experimental work has been done by Leonard [49] to construct a relationship which he considers represents the reaction rate between O_2 and MEA in the presence of either CO_2, SO_2 or both.

$$Rx_{O_2} = -5.35 \times 10^5 e^{\frac{-41.730}{RT_l}}([O_2] \times 10^{-3})^{1.46} \tag{2.64}$$

Rx_{O_2} rate of oxidative degradation mol m^{-3}

The value for the activation energy is given in J mol^{-1} and the pre-exponential unit is (mol L^{-1} s^{-1})(mol L^{-1})$^{-1.46}$. Since MEA is always in excess, its influence on the oxidative degradation can be assumed constant. This reaction rate has been incorporated into the dynamic model, which allows it to predict the amount of MEA which has been involved in the formation of degradation products but does not tell us what the degradation products are.

2.3 Energy Transfer

2.3.1 Liquid Phase

The change in the heat balance in the liquid is a result of several factors. These include the energy change from the bulk flow of the liquid, the heat transfer between the phases and the heat generated by the reactions. Other factors, such as friction are assumed to be sufficiently low that they can be ignored [34]. The factors considered in this model are:

1. **Change in energy content due to the movement of the bulk liquid**

   The temperature of the liquid is T_l, (K). The velocity of the liquid is u_l, $(\mathrm{m\ s^{-1}})$ and the flow of liquid is regarded as occurring in a negative direction.

$$-u_l \frac{\partial T_l}{\partial z} \tag{2.65}$$

2. **Transfer of energy at the interface of the phases**

   The energy transfer at the interface of the phases is driven by the temperature difference between the vapour and liquid phases and can be written

$$\frac{h_T a_{wl}(T_g - T_l)}{LC_{pl}} \tag{2.66}$$

   h_T heat transfer coefficient W m^2 K
   The Chilton-Colburn analogy is applied to obtain the heat transfer coefficient in the gas phase [12]. The heat transfer between the liquid and the gas is controlled by the resistance to heat transfer in the gas phase as the resistance to heat transfer in the gas is much greater than that in the liquid.

$$h_T = K_g \left(\frac{\rho_g C_{pg} \lambda^2}{D_g^2} \right)^{1/3} \tag{2.67}$$

K_g	mass transfer coefficient in the gas	m s^{-1}
ρ_g	density of the gas	kg m^{-3}
λ	thermal conductivity of gas	W m^{-1} K^{-1}
D_g	diffusivity of the gas	m^2 s^{-1}

3. **Transfer of energy due to the flux of the components from one phase to another**

   In this model, the components that are considered to move between phases are CO_2, O_2, MEA and H_2O. When a component transfers from one phase to the other it takes with it a body of energy which is at a different temperature to the recipient phase. Thus the temperature of both phases is changed by the transfer. CO_2 and O_2 diffuse from the vapour to the liquid, MEA

evaporates into the vapour phase and H_2O moves from one phase to the other depending on the conditions in the absorber column.

$$\frac{a_{wl}(T_g - T_l)\sum N_i C_{pi}}{LC_{pl}} \tag{2.68}$$

i represents components CO_2, O_2, H_2O or MEA

4. **Change in energy due to the phase change of components**

This model includes the evaporation of MEA and the vaporisation and condensation of H_2O which results in the change of heat in the vapour and the liquid.

$$\frac{a_{wl}(N_{CO_2}\Delta H_{absCO_2} - N_{MEA}\Delta H_{vapMEA} - N_{H_2O}\Delta H_{vapH_2O} - N_{O_2}\Delta H_{absO_2})}{LC_{pl}} \tag{2.69}$$

ΔH_{absCO_2}	latent heat of absorption of CO_2	J mol^{-1}
ΔH_{absO_2}	latent heat of absorption of O_2	J mol^{-1}
ΔH_{vapMEA}	latent heat of vaporisation of MEA	J mol^{-1}
ΔH_{vapH_2O}	latent heat of vaporisation of H_2O	J mol^{-1}

5. **Change of energy due to reaction**

There are two main equations under consideration. One is the overall reversible reaction between MEA and CO_2 where MEA is in great excess, equation (2.54). This drives the equilibrium to the right at absorber temprature and results in the formation of the carbamate compound. This equation has been modeled previously as the mechanism kinetics of the reaction are well known and is the basis of the absorption/desorption process. The other equation which must be considered is that between MEA and O_2, (2.60). Both of these reactions are exothermic and contribute to the change in energy content

$$\frac{d_H}{LC_{pl}} \tag{2.70}$$

where d_H is the amount of heat generated by the reactions included in the model (J m^{-3}). d_H is equal to the moles of component per cubic metre,

multiplied by the energy (in Joules) produced for each mole of component generated by the reaction.

$$d_H = \sum Rx_i \Delta H_{Rxi} \tag{2.71}$$

i CO_2 or O_2

2.3.2 Vapour Phase

The energy balance for the vapour phase is similar to the liquid phase except that there is no heat generated from reactions or from change of state of any component as they occur in the liquid phase only [32, 72]. The heat transfer term in the vapour phase is constructed similarly to that in the liquid phase. The factors to consider are:

1. **Change in energy content due to the movement of the vapour through the column**

   The temperature of the vapour in the column is T_g and the velocity is u_g.

   $$-u_g \frac{\partial T_g}{\partial z} \tag{2.72}$$

2. **Transfer of energy at the interface of the phases**

   This is equivalent to the term in the differential equation for the liquid phase but the heat is transferred in the opposite direction.

   $$\frac{h_T a_{wg}(T_l - T_g)}{GC_{pg}} \tag{2.73}$$

3. **Transfer of energy due to the flux of the components from one phase to another**

   MEA moves from the liquid to the vapour phase while CO_2 and O_2 diffuse in the reverse direction. H_2O can diffuse in either direction and is dependent on the properties of the two phases at the point in the column.

   $$\frac{a_{wg}(T_l - T_g)(N_{MEA}C_{pMEA} + N_{CO_2}C_{pCO_2} + N_{O_2}C_{pO_2})}{GC_{pg}} + \frac{a_{wg}(T_l - T_g)N_{H_2O}C_{pH_2O}}{GC_{pg}} \tag{2.74}$$

2.3.3 Total Moles

Working in mole fractions has required the use of the flow rate of the liquid and the gas in moles. As the composition of the two phases change with time it is necessary to include a PDE for both the change in the total moles of the liquid and that of the gas. See equations 2.88 and 2.89.

2.3.4 The Mathematical Model

The set of fifteen PDE's for the model are as follows:

$$\frac{\partial C_{lCO_2}}{\partial t} = -u_l \frac{\partial C_{lCO_2}}{\partial z} + \frac{N_{lCO_2} a_{wl}}{L} + \frac{Rx_{CO_2}}{L} \tag{2.75}$$

$$\frac{\partial C_{lMEA}}{\partial t} = -u_l \frac{\partial C_{lMEA}}{\partial z} + \frac{N_{lMEA} a_{wl}}{L} + \frac{Rx_{MEA}}{L} \tag{2.76}$$

$$\frac{\partial C_{lH_2O}}{\partial t} = -u_l \frac{\partial C_{lH_2O}}{\partial z} + \frac{N_{lH_2O} a_{wl}}{L} + \frac{Rx_{H_2O}}{L} \tag{2.77}$$

$$\frac{\partial C_{lMEACOO}}{\partial t} = -u_l \frac{\partial C_{lMEACOO}}{\partial z} + \frac{Rx_{MEACOO}}{L} \tag{2.78}$$

$$\frac{\partial C_{lMEAH}}{\partial t} = -u_l \frac{\partial C_{lMEAH}}{\partial z} + \frac{Rx_{MEAH}}{L} \tag{2.79}$$

$$\frac{\partial C_{lO_2}}{\partial t} = -u_l \frac{\partial C_{lO_2}}{\partial z} + \frac{N_{lO_2} a_{wl}}{L} + \frac{Rx_{O_2}}{L} \tag{2.80}$$

$$\frac{\partial C_{lOP}}{\partial t} = -u_l \frac{\partial C_{lOP}}{\partial z} + \frac{N_{lOP} a_{wl}}{L} + \frac{Rx_{OP}}{L} \tag{2.81}$$

$$\frac{\partial T_l}{\partial t} = -u_l\frac{\partial T_l}{\partial z}+\frac{h_T a_{wl}(T_g - T_l)}{LC_{pl}}+\frac{a_{wl}(T_g - T_l)(N_{CO_2}C_{pCO_2} + N_{MEA}C_{pMEA} + N_{O_2}C_{pO_2})}{LC_{pl}}$$
$$+\frac{a_{wl}(N_{CO_2}\Delta H_{absCO_2} - N_{MEA}\Delta H_{vapMEA} - N_{H_2O}\Delta H_{vapH_2O} - N_{O_2}\Delta H_{absO_2})}{LC_{pl}}$$
$$+\frac{a_{wl}(T_g - T_l)N_{H_2O}C_{pH_2O}}{LC_{pl}} + \frac{d_H}{LC_{pl}} \quad (2.82)$$

$$\frac{\partial C_{gCO_2}}{\partial t} = u_g\frac{\partial C_{gCO_2}}{\partial z} - \frac{N_{gCO_2}a_{wg}}{G} \quad (2.83)$$

$$\frac{\partial C_{gMEA}}{\partial t} = u_g\frac{\partial C_{gMEA}}{\partial z} - \frac{N_{gMEA}a_{wg}}{G} \quad (2.84)$$

$$\frac{\partial C_{gH_2O}}{\partial t} = u_g\frac{\partial C_{gH_2O}}{\partial z} - \frac{N_{gH_2O}a_{wg}}{G} \quad (2.85)$$

$$\frac{\partial C_{gO_2}}{\partial t} = u_g\frac{\partial C_{gO_2}}{\partial z} - \frac{N_{gO_2}a_{wg}}{G} \quad (2.86)$$

$$\frac{\partial T_g}{\partial t} = u_g\frac{\partial T_g}{\partial z}+\frac{h_T a_{wg}(T_l - T_g)}{GC_{pg}}+\frac{a_{wg}(T_l - T_g)(N_{CO_2}C_{pCO_2} + N_{MEA}C_{pMEA} + N_{O_2}C_{PO_2})}{GC_{pg}}$$
$$+\frac{a_{wl}(T_g - T_l)N_{H_2O}C_{pH_2O}}{GC_{pg}} \quad (2.87)$$

$$\frac{\partial L}{\partial t} = -u_l\frac{\partial L}{\partial z} + a_{wl}(N_{CO_2} + N_{H_2O} + N_{O_2} + N_{MEA})$$
$$+ Rx_{CO_2} + Rx_{MEA} + Rx_{MEAH} + Rx_{MEACOO} + Rx_{O_2} + Rx_{OP} \quad (2.88)$$

$$\frac{\partial G}{\partial t} = u_g\frac{\partial G}{\partial z} - a_{wg}(N_{CO_2} + N_{H_2O} + N_{O_2} + N_{MEA}) \quad (2.89)$$

The boundary conditions are the number of moles of MEA, H_2O, O_2 and CO_2 in the flue gas, MEA, H_2O, $MEAH^+$, $MEACOO^-$ and OP in the solvent entering the columnn, the input temperatures of the liquid and the gas and the total number of moles in the liquid phase and in the vapour phase. The vapour and liquid leaving the column are free boundaries. The initial conditions are the number of moles, both vapour and liquid, of O_2, CO_2, MEA, $MEAH^+$, $MEACOOH^-$ and H_2O in the column at t=0, the temperatures of the liquid and the gas in the column and the total number of moles in the liquid phase and in the vapour phase in the column.

Chapter 3

Solving the Model

3.1 Constructing a Numerical Model

The dynamic model has two independent variables, column height and time, and is a system of partial differential equations (PDEs). Modern computing has made it possible for dynamic models to incorporate factors which vary with column height and time such as density, mass transfer rates, reaction rates and viscosity. The dynamic model does not assume the system is in steady state.
This model is adapted from a system of advection-diffusion-reaction equations [30]. Due to the assumptions listed in Section 2.1, there is no requirement for a diffusion term in either phase, nor a reaction term in the vapour phase. As there is movement of components across the liquid/gas interface there is a term to account for the flux between phases. Hence, the liquid phase becomes an advection-reaction system with a term for the flux of components and the gaseous phase is an advection system plus a flux term. PDEs were used to describe the time and space dependent variables (concentration, temperature) of the absorber column. The mathematical problem arising from the resulting dynamic absorber model is a boundary value problem (BVP). To solve this problem, the height dimension is discretized to give an ordinary differential equation (ODE) in the variable time, at various discrete height values. The ODEs formed can then be solved using MATLAB ode15s solver. With the two phases running counter currently, the boundary conditions for the liquid are known at the top of the absorber and those for the vapour at the bottom. The boundary values for the system are given by the inlet compositions, the temperatures, and the flow rates of the liquid and gas phases. It is assumed that initially the absorber column contains the flowing solvent and void vapour space and the flue gas is released into the bottom of the column.
One algorithm required to solve these types of problems is the finite difference

method [83]. For the work in this thesis, both the backward and forward finite difference methods have been employed to integrate for the height variable while the MATLAB ode15s solver has been used for the numerical solution of the time variable. The height of the column, z, is discretized into a vertical step size of Δz with each discrete height denoted by $x\Delta z$ where $1 \leq x \leq n$. Then the spatial partial derivatives are approximated by either the forward or backward difference method which produces a series of ODE's as shown in equations 3.1 to 3.6. Equations 3.1, 3.2 and 3.6 use the forward method and equations 3.3, 3.4 and 3.5 employ the backward method. The value of the gas concentration of component i at point $x\Delta z$ is a function only of the variable t and is denoted by $C_{g,i,x}(t)$ with $1 \leq x \leq n$. Similarly, the liquid concentration of each component at point $x\Delta z$ is $C_{l,i,x}(t)$ with $1 \leq x \leq n$. The boundary condition for the gas is given by $C_{g,i,1}(t)$ and for the liquid $C_{l,i,n}(t)$. The initial conditions are $C_{g,i,x}(0)$ and $C_{l,i,x}(0)$. Equation 2.2 can be re-written as

$$\frac{dC_{g,i,x}}{dt} = u_g \left(\frac{C_{g,i,x} - C_{g,i,x-1}}{\Delta z} \right) + \frac{a_{wg,x} N_{i,x}}{G_x} \tag{3.1}$$

for $2 \leq x \leq n$. Using the forward difference method again to approximate the spatial derivative, an expression for the temperature change in the gas is obtained. This is the numerical version of equation (2.6).

$$\frac{dT_{g,x}}{dt} = u_g \left(\frac{T_{g,x} - T_{g,x-1}}{\Delta z} \right) + \frac{a_{wg,x} h_T (T_{g,x} - T_{l,x})}{G_x C_{pg,x}} + \frac{a_{wg,x} \sum N_{i,x} C_{pi,x} (T_{g,x} - T_{l,x})}{G_x C_{pg,x}} \tag{3.2}$$

for $2 \leq x \leq n$. For liquid concentration and temperature, the backward difference method is used to approximate the spatial partial derivative because the boundary conditions for the liquid phase at the top of the column, where $x = n$, are known. Equation (2.1) is approximated for $1 \leq x \leq n-1$ by the equation

$$\frac{dC_{l,i,x}}{dt} = -u_l \left(\frac{C_{l,i,x+1} - C_{l,i,x}}{\Delta z} \right) + \frac{a_{wl,x} N_{i,x}}{L_x} + Rx(C_{l,i,x}, T_{l,x}, L_x) \tag{3.3}$$

For equation (2.5) the equation becomes

$$\frac{dT_{l,x}}{dt} = -u_l \left(\frac{T_{l,x+1} - T_{l,x}}{\Delta z} \right) + \frac{a_{wl,x} h_T}{L_x C_{pl,x}} (T_{l,x} - T_{g,x}) + \frac{a_{wl,x} \sum N_{i,x} C_{pi,x} (T_{l,x} - T_{g,x})}{L_x C_{pl,x}} + \frac{d_H}{L_x C_{pl,x}} + \frac{a_{wl,x} (T_{l,x} - T_{g,x}) \sum Ni \Delta H_i}{L_x C_{pl,x}} \tag{3.4}$$

The two additional equations that represent the change in concentration (mole m^{-3}) of the liquid and the gas phases are:

$$\frac{dL_x}{dt} = -u_l \left(\frac{L_{x+1} - L_x}{\Delta z} \right) + \frac{a_{wl,x} \sum N_{i,x}}{L_x} + \frac{\sum Rx_x}{L_x} \tag{3.5}$$

$$\frac{dG_x}{dt} = u_g \left(\frac{G_x - G_{x-1}}{G_x} \right) - \frac{a_{wg,x} \sum N_{i,x}}{G_x} \tag{3.6}$$

MATLAB ODE15s was chosen to solve the system of ODE's. A time increment, Δt, is assigned so that $t = j\Delta t$ becomes a discretization of the time variable for which MATLAB reports the values $C_{l,i,x}(j\Delta t) = C_{l,i,x,(j)}$. This method can proceed successively to calculate all variables at time increment $j + 1$ from those already calculated at time increment j.

Stability of the numerical solution is guaranteed if we let $\Delta t = \min \left\{ \frac{\Delta z}{v_g}, \frac{\Delta z}{v_l} \right\}$ since both Courant-Friedrich-Lewy numbers, $v_g \frac{\Delta t}{\Delta z}$ and $v_l \frac{\Delta t}{\Delta z}$, must be less than 1 [28].

3.2 Validating the Model

The model is validated with real data from a retro-fitted pilot plant at the AGL Loy Yang power plant. This retro fitted pilot plant is used to quantify the degradation of MEA and thus the rate of accumulation of oxidation products. This pilot plant has the absorption section split into two absorber columns connected in series. The two sections are joined with piping that was not lagged during the data collection period and, as a result, the temperature profiles contain a discontinuity in the data. The impact of this temperature change on the concentrations of the gas and the liquid is minimal. In order to confirm that the model is a true representation of the behaviour of the temperature and the absorption of CO_2 and could be used to quantify the oxidation of MEA, the model is initially validated against experimental results from the single laboratory absorber column at the CSIRO Energy Flagship at Newcastle. This column does not have the disjoint in the temperature but it also does not have O_2 as an input so there are no experimental results to indicate the change in the MEA concentration from oxidative degradation. This aspect of the model can not be tested.

3.2.1 Validating Model with CSIRO Laboratory Column

The laboratory column at the CSIRO laboratory in Newcastle is a stand alone column with constant input of both gas and liquid. The input gas contains known concentrations of CO_2, H_2O and N_2 and the input solvent known concentrations of MEA and H_2O. The column consists of nine 0.3m sections of random packing alternating with eight 0.3m void sections where parameters such as temperature and concentration can be measured. The top section of packing is used as a demister and is above the solvent input which means that only the bottom eight sections of packing are involved in the absorption system. The total height of the random packing for absorption and the void sections is 4.8m. Using the physical properties

of the column and the packing, it was determined that the surface area available for absorption in the void sections was equivalent to 0.665% of the total surface area and this was considered to be insignificant in the absorption calculations. The height of packing available for absorption of gas was 2.4m. The packing used is 16mm stainless steel Pall rings. Tests were conducted with the concentrations of

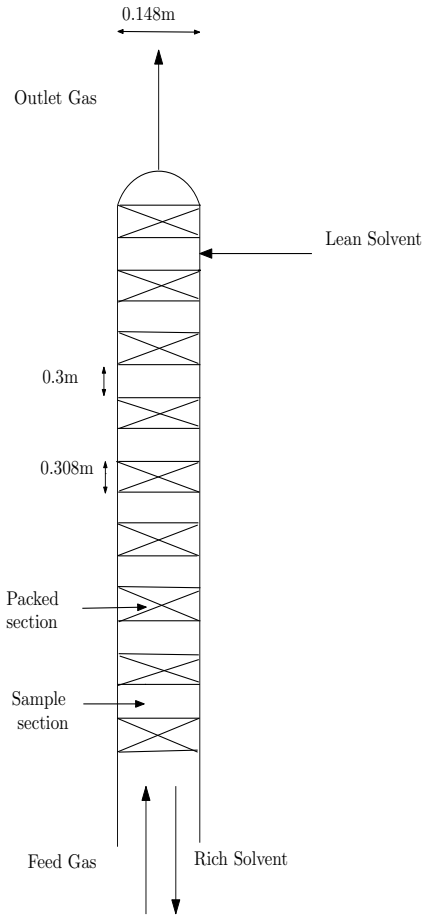

Figure 3.1: Newcastle laboratory absorber column

both inputs being held constant during each run but varying between runs. The concentration of the CO_2 in both inlet and outlet streams was determined and used to validate the model for CO_2 absorption. The absorber was run with input liquid to input gas concentration ratios (L/G) ranging from 2.30 to 9.35. The system was assumed to be adiabatic. Influences such as the characteristics of the internal packing used in the column are included in the model. As there is no pressure build up, the input phase velocities are regarded as constant. The parameters, experimental data and the resulting graphs for two sets of data that were used for

validation of the model have been included here. Although the laboratory column did not produce data to indicate the accumulation of oxidation products and could not be used to validate the degradation of MEA, it was used to validate the model for CO_2 absorption. See Figures 3.2 and 3.3 and Appendix A.

Figure 3.2 shows the temperature and CO_2 profiles for data Run A, where L/G is 9.35 and Figures 3.3 are for Run B with L/G of 4.214. These profiles are representative of the system 30 minutes after it has reached a pseudo steady state (which takes from 2 to 5 minutes). The solid line represents the average temperature of the vapour and the liquid from this developed model, the blue dotted line is the model produced by Saimpert et al [71] (a rate-based model for the Newcastle column) and the red dots represents the temperature from the experimental results from the CSIRO laboratory column. The model data in the two temperature graphs produced follows the experimental data and shows superior correlation to that of Saimpert et al. The movement of the position of the temperature bulge follows the findings of Kvamsdal [46] who found that if the L/G ratio is higher, the bulge tends to the base of the column and a lower L/G ratio means the bulge moves towards the top of the column. The temperature maximum in Run A (with the higher L/G ratio) occurs at a column height of 0.22m while that of Run B occurs at 0.65m. This is another indication that the model is performing as expected. One factor that could explain the small discrepancies between the simulated temperature curve and the experimental curve is the unavailability of packing constants (C_v, C_l, C_h) for the 16mm metal Pall ring packing used in the absorber column. Packing constant data for 25mm metal Pall ring packing was used for the model. The temperature curve in Figure 3.2 is slightly higher than the experimental results as the column is assumed to be adiabatic even though some heat loss from the system would be expected. In Figure 3.3 with the lower L/G, the temperature peak moves up the column due to the shift in the position of greatest absorption. It would be expected that the temperature bulge would move further up the column but the differences in the curves are within an acceptable error margin. The standard error of the residuals, RSE, for the model temperature curve is 4.88°.
The graphs for the absorption of CO_2 show good correlation with Run A having a RSE of 0.008 mole fraction and correlation coefficient, R, of 0.837 while Run B has a RSE of 0.011 mole fraction and R of 0.969. This is interpreted as strong correlation between the experimental data and the model data. The concentration of the CO_2 at 0.21 m in the column in both runs was contaminated with extra water due to a fault in the sampling system and thus is lower than it should be. From the above results and discussion, it was concluded that the model was a good represention of the single absorber column and could be applied with some

a)

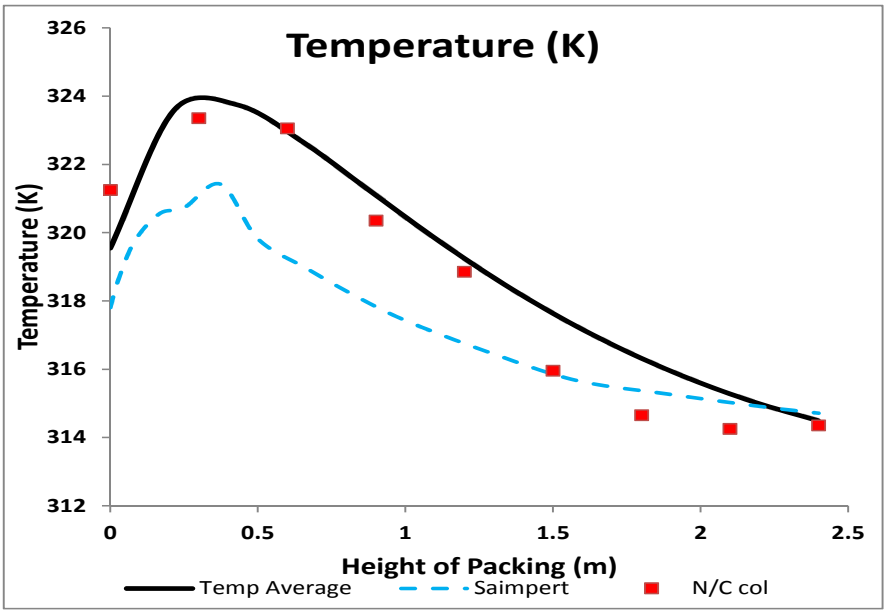

b)

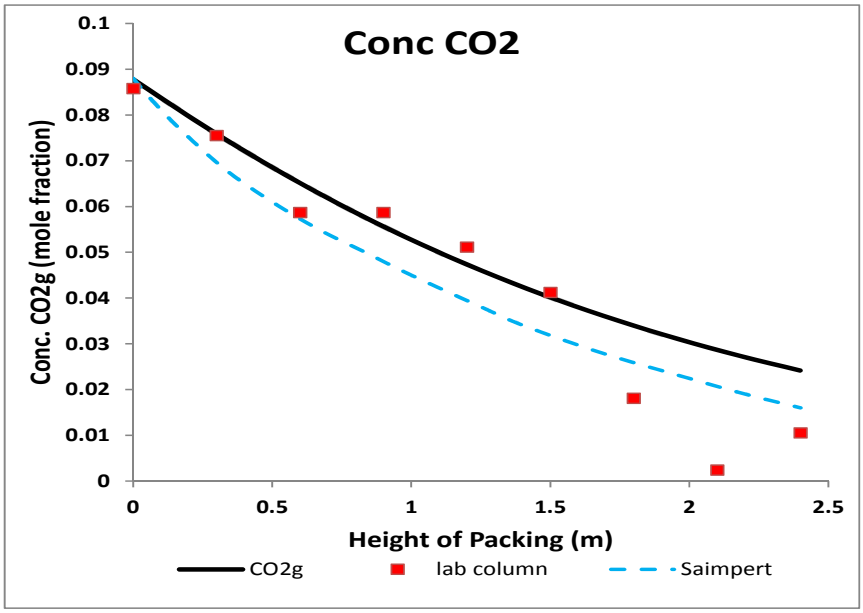

Figure 3.2: Profile for a) temperature and b) CO_2 absorption, Run A, Newcastle

confidence to the more complex split absorber column in the pilot plant at Loy Yang power plant.

a)

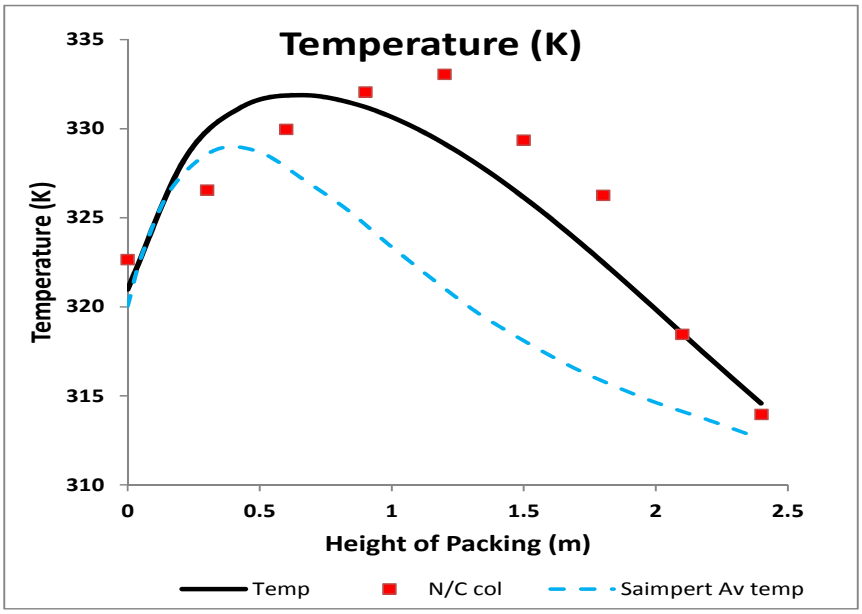

b)

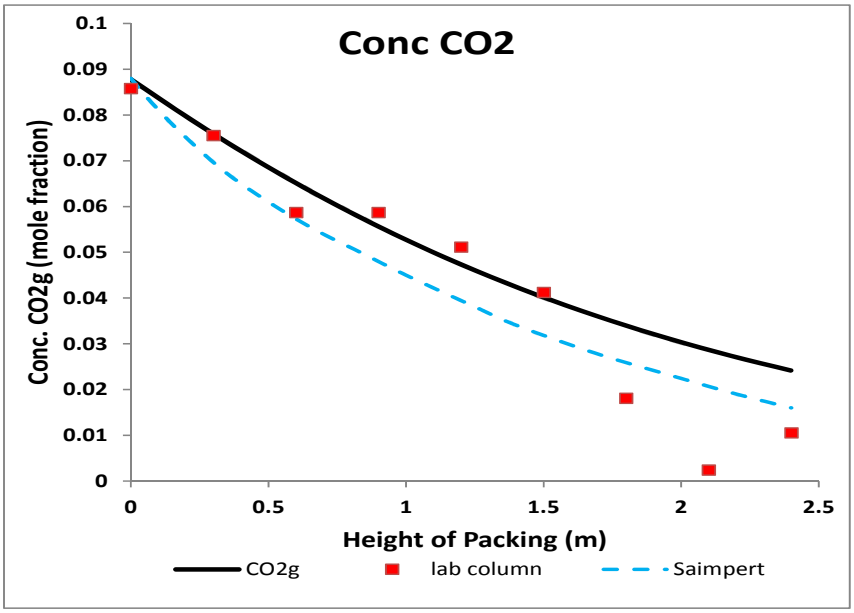

Figure 3.3: Profile for a) temperature and b) CO_2 absorption, Run B, Newcastle

3.2.2 Validating Model with CSIRO Retro-fitted Pilot Plant

CSIRO has retro-fitted a CO_2 capture pilot plant to the lignite-fuelled power station at AGL Loy Yang in Victoria and the industrial flue gas is fed directly from the

power station into the pilot plant. The pilot plant consists of two absorber columns connected in series, both containing two sections of 1.35m of random packing with a small void section in between to cater for temperature measurements. There is also a solvent make-up tank (or feed tank) which is included in this model. They are part of a complete system which includes a desorber, heat exchanger, reboiler, condenser and other necessary equipment that are not part of this mathematical model. The gas is fed into a pretreatment section where the sulphur and nitrogen oxides and any particulates are removed before proceeding to the bottom of the first absorber column, ABS2. The input flue gas to the base of this column consists

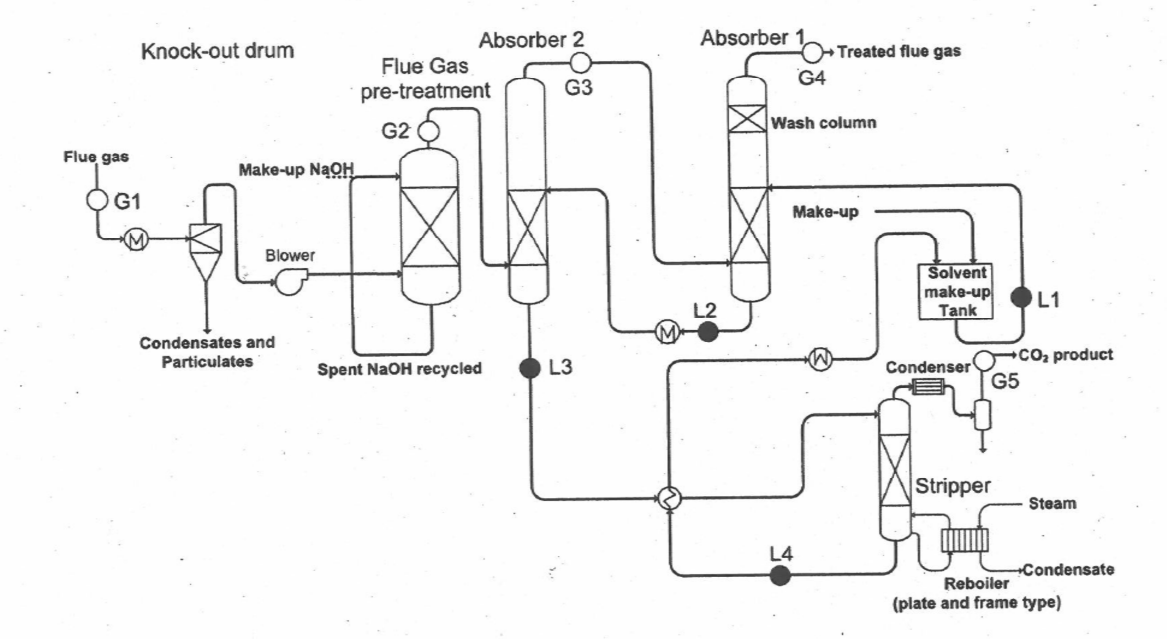

Figure 3.4: Simplified process flow diagram at CSIRO PCC pilot plant at AGL Loy Yang[5]

of known concentrations of H_2O, N_2, CO_2 and O_2. The input solvent is fed into the top of the second absorber column, ABS1, and runs counter currently to the gas feed. It consists of H_2O, MEA, some residual carbamate compounds and oxides of the solvent which were not removed in the desorber. (Further details of the pilot plant operation can be obtained from Cottrell et al and Artanto et al. [5, 20].) The temperature was recorded by thermocouples inserted in the void sections of

each column and is an average temperature of vapour and liquid rather than measured individual phases. As the columns were at low temperatures (about 323°K) radiation losses from the thermocouple tips can be regarded as insignificant and any uncertainties in reading were inherent calibration errors only. For this study the concentration of the input gas from the pretreatment section is assumed to be constant. That of the liquid solvent varies as the modelling proceeds. The model has been validated with data from the AGL pilot plant which has temperature measurements at the inlet and outlet to each column as well as in the void section between the packing. The concentration of the components in the input and output liquid and gas for each absorber column is also known. This work does not consider operational changes as other authors have reported on the effect of variable operations on an absorption pilot plant [9, 15, 27, 39].
The packing used in the absorber columns is 25mm stainless steel Pall rings and the associated constants were obtained from Billet and Schultes [10]. Unlike the Newcastle column, this PCC pilot plant did produce data which included inputs and outputs of oxygen. This data was used to validate the model for both CO_2 absorption and, indirectly, for the degradation of MEA. While operating the CSIRO PCC pilot plant at AGL Loy Yang, it was found that water was lost during the cycle and there was a need to top up the volume in the feed tank. This additional water is not measured accurately during operation of the plant but it is necessary to keep the total volume of the liquid phase constant. The replaced water was slug-dosed on an ad hoc basis, but the model incorporates it as a continuous make-up feed. This water loss is thought to occur due to evaporation in the desorber. The amount of H_2O lost from the solvent each cycle was determined from a mass balance around the feed tank. The total MEA in the liquid at the bottom of the absorber is as follows.

$$C_{MEA,tot,j} = C_{MEAl,1,j} + C_{MEACOOl,1,j} + C_{MEAHl,1,j} \tag{3.7}$$

where $C_{MEA,tot,j}$ is the total mole fraction of MEA at time j.
As the CO_2 removed in the stripper should match the loading in any particular run, the ratio $C_{MEACOOl}$ to $C_{MEA,tot}$ will be constant for that run. The moles of the five components of the solvent entering the feed tank is represented by the following equations.

$$MEA_{s,j} = \left(1 - 2\frac{C_{MEACOOl,i}}{C_{MEA,tot,i}}\right)\ C_{MEA,tot}\ V_l\ \Delta t \tag{3.8}$$

$$MEACOO_{s,j} = \left(\frac{C_{MEACOOl,i}}{C_{MEA,tot,i}}\right)\ C_{MEA,tot}\ V_l\ \Delta t \tag{3.9}$$

$$MEAH_{s,j} = \left(\frac{C_{MEACOOl,i}}{C_{MEA,tot,i}}\right)\ C_{MEA,tot}\ V_l\ \Delta t \tag{3.10}$$

$$H_2O_{s,j} = mH_2O_{(1,j)}\ V_l\ \Delta t \tag{3.11}$$

$$OP_{s,j} = mOP_{(1,j)}\ V_l\ \Delta t \tag{3.12}$$

where $\mathrm{MEA}_{s,j}$, $\mathrm{MEACOO}_{s,j}$, $\mathrm{MEAH}_{s,j}$, $\mathrm{H_2O}_{s,j}$ and $\mathrm{OP}_{s,j}$ represent the moles of each component as they leave the stripper. $\mathrm{C}_{MEACOOl,i}$ and $\mathrm{C}_{MEA,tot,i}$ are the initial mole fractions of MEACOO and total MEA in the liquid phase. V_l is the flow of the liquid in moles per second obtained by multiplying the constant mass flow rate with the density of the solution as it leaves the absorber. dt is the time step which is the minimum absolute value of the two variables, $\frac{dz}{u_G}$ and $\frac{dz}{-u_L}$. The discrepancy noted in the mole balance around the feed tank was taken to be equal to the amount of water added at the feed tank and is expressed as $\mathrm{H_2O}_{ex}$.

The focus of this work is to produce a model of the absorption column that will predict the degradation rates of MEA and, as a consequence, the accumulation rates of oxidation products (OP) in the solvent as it circulates throughout the absorption/desorption system. Previously, degradation has been quantified by the evolution of ammonia, not oxygen consumption, however oxidative degradation can occur without the production of NH_3 or the NH_3 can be consumed in a further reaction [33]. An example of this is the formation of oxalic acid followed by oxalamide.

$$HOC_2H_4NH_2 + 2O_2 \rightarrow H_2C_2O_4 + NH_3 + H_2O \tag{3.13}$$

$$HOC_2H_4NH_2 + 2O_2 + NH_3 \rightarrow C_2H_4N_2O_2 + 3H_2O \tag{3.14}$$

Using NH_3 as an indication of oxidative degradation results in lower levels of oxidation products being predicted than actually occur.

The oxidation products that exit the absorber column are heat stable salts which pass through the desorber unaltered and proceed to the feed tank. As the moles of oxidation products increase over time, the concentration of available MEA decreases. The exact oxidation reactions are unknown and the three reactions that are thought to be most likely [7, 8, 70, 88] have stoichiometry of 0.5, 1 and 2, (refer to equations (2.61) to (2.63)), so for this model the stoichiometry of the oxidation reactions was taken as 1 MEA: 1 OP. The accumulation of the oxidation products does not effect the degradation rate of MEA [33].

The number of moles of MEA in the feed tank at time $(j+1)$ is equal to the moles of MEA in the feed tank at time j, plus the moles of MEA entering the feed tank from the stripper from time j over the increment Δt, less the concentration of MEA that left the feed tank at time j. nV_{ft} is the total moles of components in the feed tank.

Similar relationships are used for the moles of $MEAH^+$, $MEACOO^-$ and oxidation products. The equation for water also includes a term for the consideration of the water loss from the system.

$$H_2O_{n,j+1} = C_{H_2On,j}\ nV_{ftn,j} + H_2Os_j - H_2O_{n,j}\ V_l\ \Delta t + H_2O_{ex} \tag{3.15}$$

H_2O_{ex} is the extra water added in replace the water lost through the system due to evaporation in the stripper and is calculated by a mole balance around the feed tank assuming constant moles in the feed tank. Each equation is then converted into mole fraction before the solvent enters into the top of the absorber. The total number of moles in the feed tank, n_{tot}, is the total moles of MEA, $MEACOO^-$, $MEAH^+$, H_2O (including additional water) and OP. The equation for MEA in mole fraction entering the top of the absorption column is:

$$C_{MEAl,n,j+1} = \frac{C_{MEAl,n,j}\ nV_{ft(n,j)} + MEAs_{n,j} - MEAl, n, j\ V_l\ \Delta t}{n_{tot}} \tag{3.16}$$

Similar equations are applied to the four other components. These relationships provide the changing boundary conditions for the liquid at the top of the column which occur due to the accumulation of the oxidation products.

Validation and Discussion Validation of the model was done with two sets of data from the AGL Loy Yang pilot plant and they have been notated as Run 280509 and Run 061011. The data was chosen with regard to the magnitude of L/G in order to have two different conditions for the verification of the work. Run 280509 has L/G of 3.97 while Run 061011 has L/G of 6.44. Run 061011 should produce a bulge in the temperature graph towards the base of the column. Greater absorption results in an increase in temperature from the exothermic reactions and this can be seen in figures 3.5 and 3.6. Initially the absorption system was modelled as one absorber column 5.4m high. Figure 3.5 and Figure 3.6 are the outputs for the gaseous CO_2 and H_2O for the two data sets and the graph of the average temperatures for the height of the column about 15 minutes after the model has reached steady state. The shape of the curves match that shown by several other papers [40, 71, 77, 85]. The squares represent the experimental data points and their temperature graph clearly shows the position of the temperature change between the two columns. The boundary conditions are the input temperatures and concentrations of the gas and the liquid. The discrepancies between the model vapour input temperatures and the experimental vapour input temperatures occur because the model is calculating with individual gas and liquid temperatures but the results are plotted using average temperatures. As well as the input values, one other data point is available at the outlet of ABS2 for CO_2 and H_2O validation. The experimental data at height 0, 1.35 and 2.65 metres in the temperature graphs are the results for the bottom, middle and top of ABS2 while the data at 2.75, 4.05 and 5.4 m are from ABS1. The model is assumed to be an adiabatic system but the experimental results indicate otherwise. The two absorber columns and the piping between them were not insulated at the time of operation. As the data came from October (Spring) and May (Winter), it would be expected that

a)

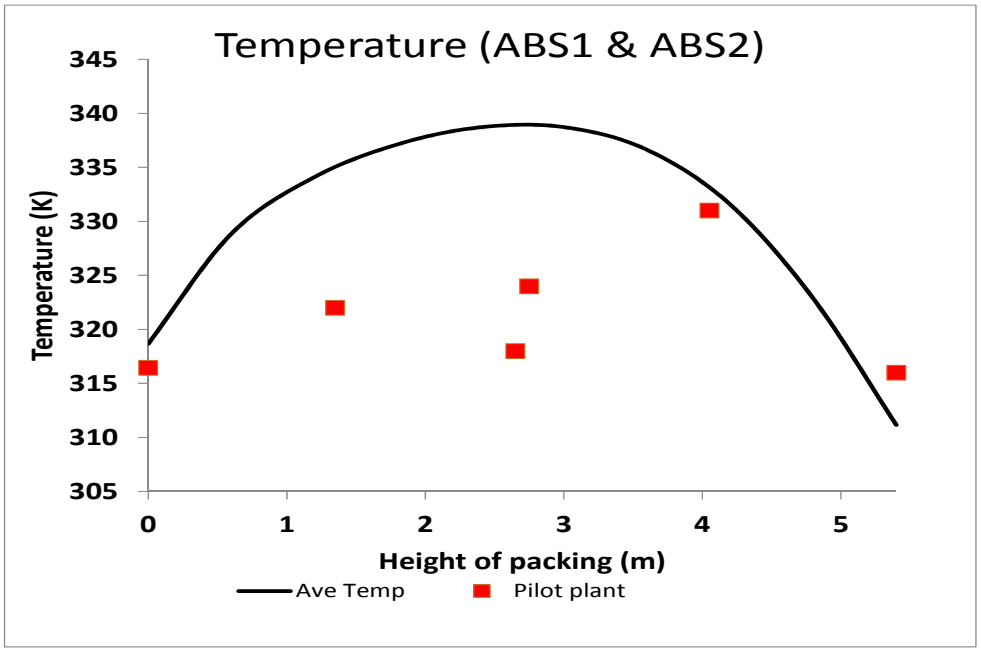

b)

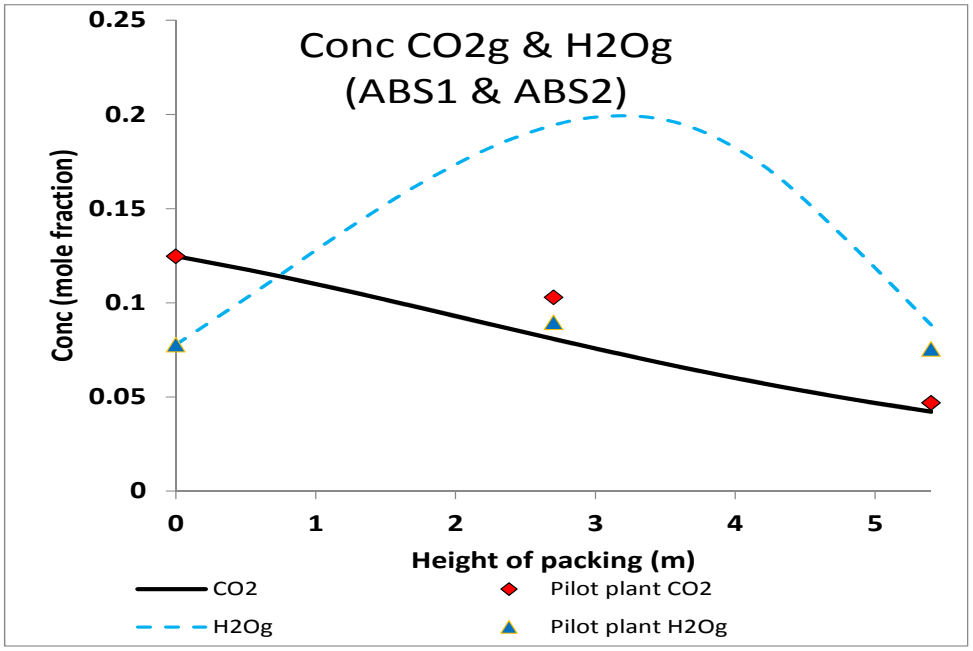

Figure 3.5: Profile for a) temperature, b) CO_2 and H_2O, ABS1 and ABS2, Run 280509, Loy Yang Pilot Plant

a)

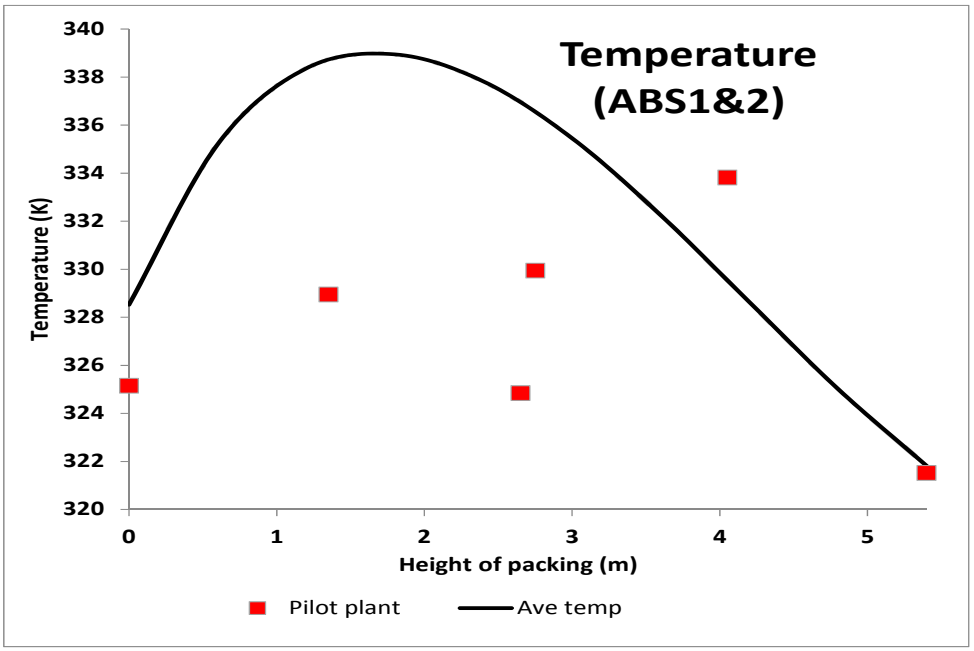

b)

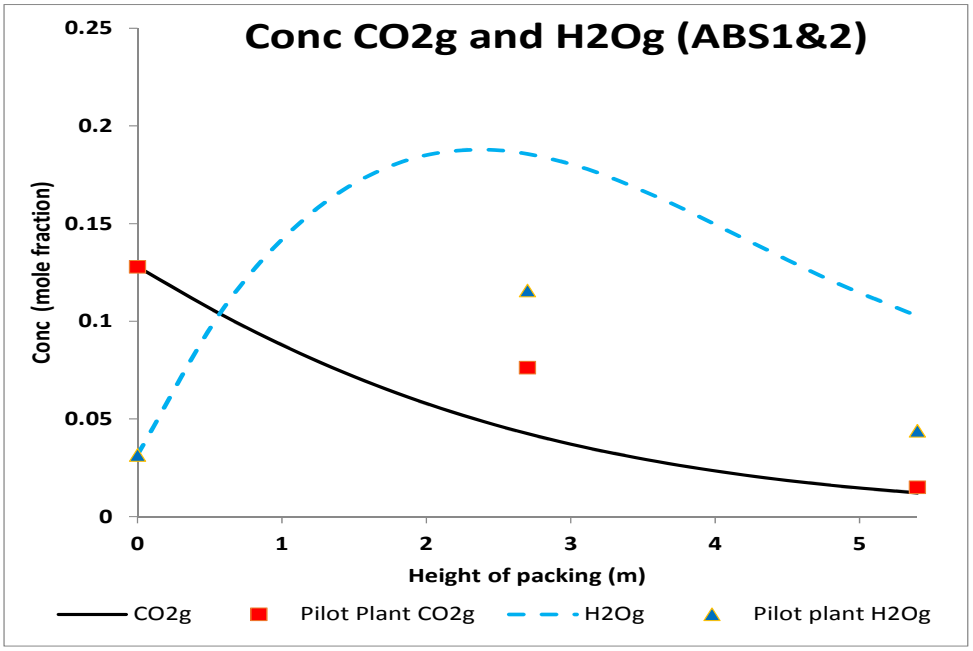

Figure 3.6: Profile for a) temperature, b) CO_2 and H_2O, ABS1 and ABS2, Run061011, Loy Yang Pilot Plant

the surrounding air temperature, which was typically 45 K lower than that of the column, would reduce the temperature of the phases as they passed through the connecting piping. The experimental data shows a temperature drop between the two absorption columns which is not evident when modeling the system as one column. Heat loss from the column may also be a factor affecting the height of the temperature bulge. This temperature dislocation between the columns will effect the absorption of the CO_2 and this may be explained by the intermediary experimental point in the graph of CO_2 absorption (Figure 3.5 and 3.6) which indicates less absorption of CO_2 at that point than is shown by the model. There model shows a final absorption reading within 10% of the experimental data for the concentration of CO_2 removed from the flue gas.

The movement of the temperature bulge towards the base of the column is as expected for data with the higher L/G ratio, Run 061011. This is also validated by the shift in the peak of the water content in the vapour phase in Figure 3.6. A higher temperature results in greater water loss from the liquid phase. Figure 3.5 and 3.6 also show the removal of CO_2 and H_2O from the gas for the total length of the packed column. The graph shows good correlation for the exit concentrations of gaseous CO_2 and H_2O despite the absorber column being operated as two separate sections. The H_2O curve for the model exhibits significant H_2O evaporation and this is in agreement with the experimental work done by Simon et al which is represented by the triangles on the graph [77]. Figure 3.7 is the graph of the temperature when the absorber in Run 280509 is modelled in two sections (but placed on one graph) and shows the experimental data points and the simulated values from the model. The shape of the temperature curve in both ABS1 and ABS2 reflects the data with the maximum value occurring at similar positions in the graph. The experimental data points of the temperature curve in ABS2 are about 8^o below the simulated curve. This is a similar result as reported in the work of Artanto et al [5] and can be attributed to the jump in temperature at the base of ABS1 of 6^o.

The graph for Run 061011, Figure 3.7, reflects the results obtained for Run 280509. The L/G ratio is higher in Run 061011 so the temperature bulge is closer to the bottom of each column. There is more liquid to absorb CO_2 as the gas enters the column which leads to a temperature increase at the bottom of the column. The temperature range in both absorber columns in this Run are $5^o - 10^o$ higher than in Run 280509.

Some parameters were altered in order to examine the effect of their change on the absorption of CO_2 and the accumulation of oxidation products. The input temperatures to the column were increased by 10^o, and also decreased by 10^o, to determine the effect this would have on the removal of CO_2 and the accumulation of oxidation products. Figure 3.8 shows that 1.6% more CO_2 is absorbed when the

a)

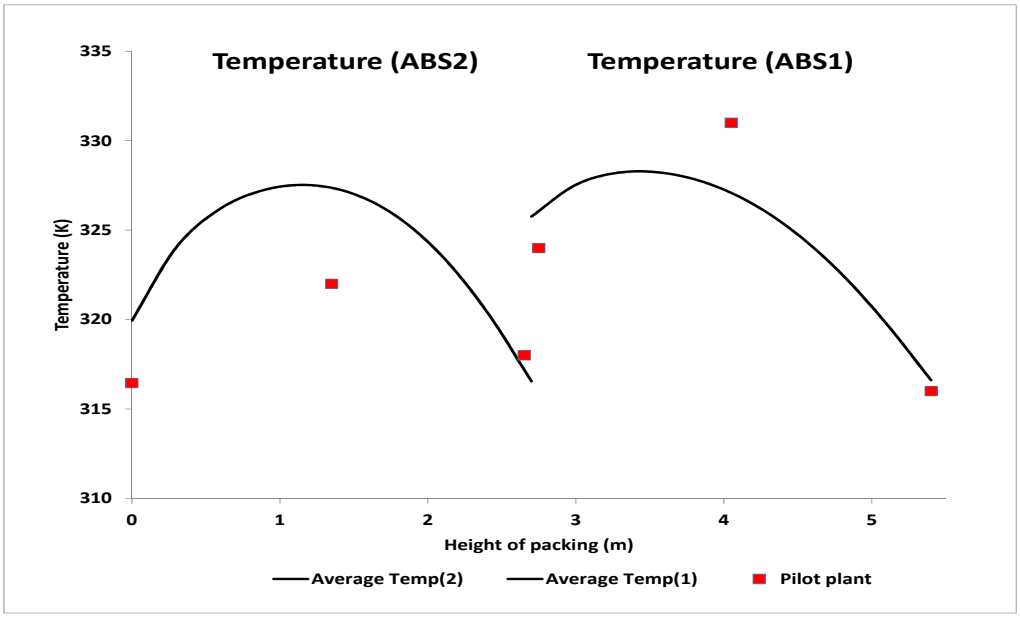

b)

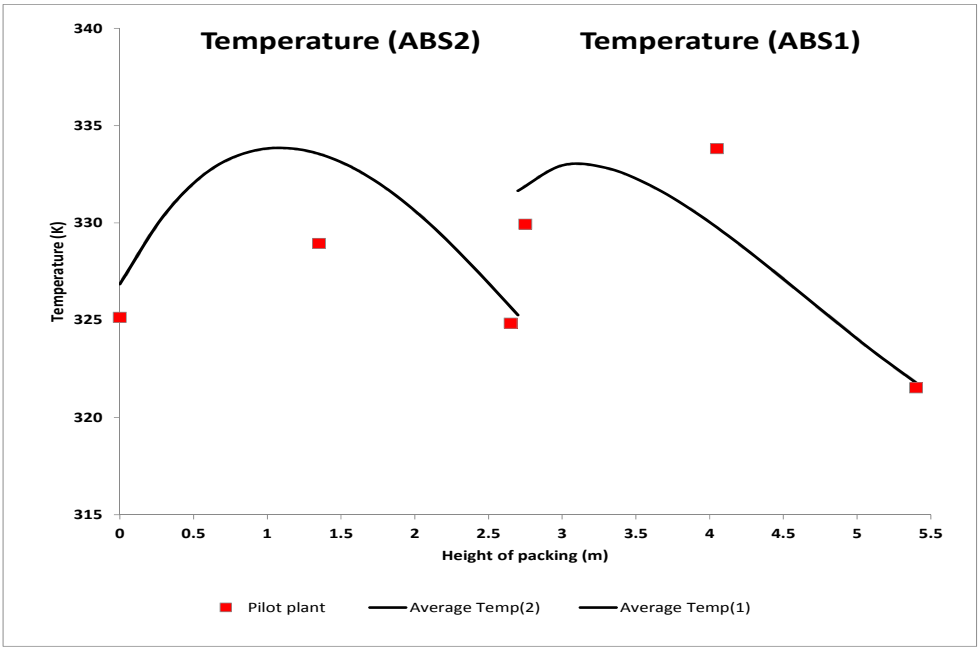

Figure 3.7: Profile for temperature, a) Run 280509 b) Run 061011, AGL Loy Yang Pilot Plant

a)

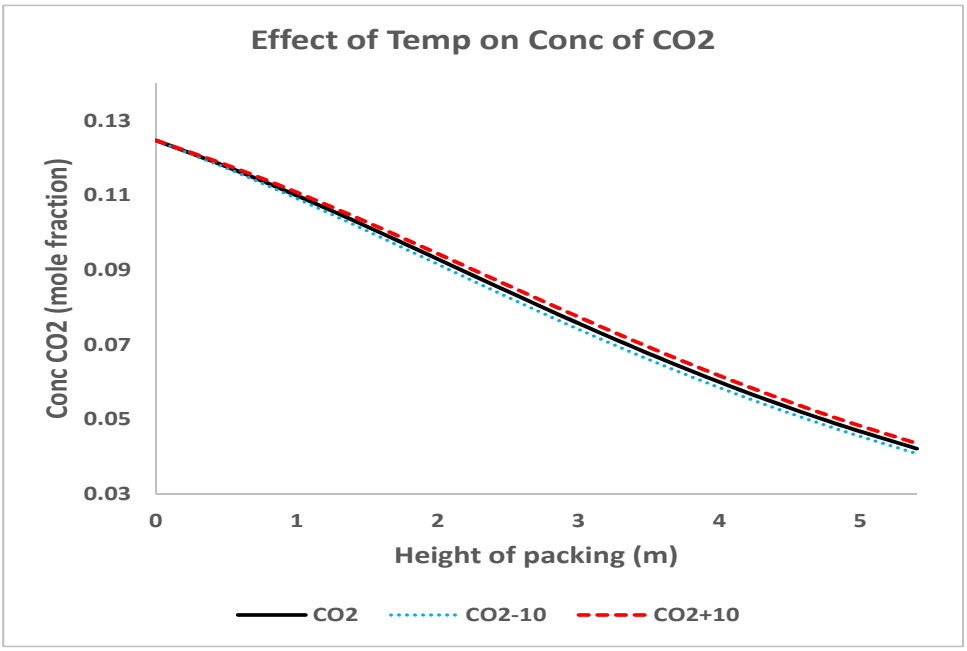

b)

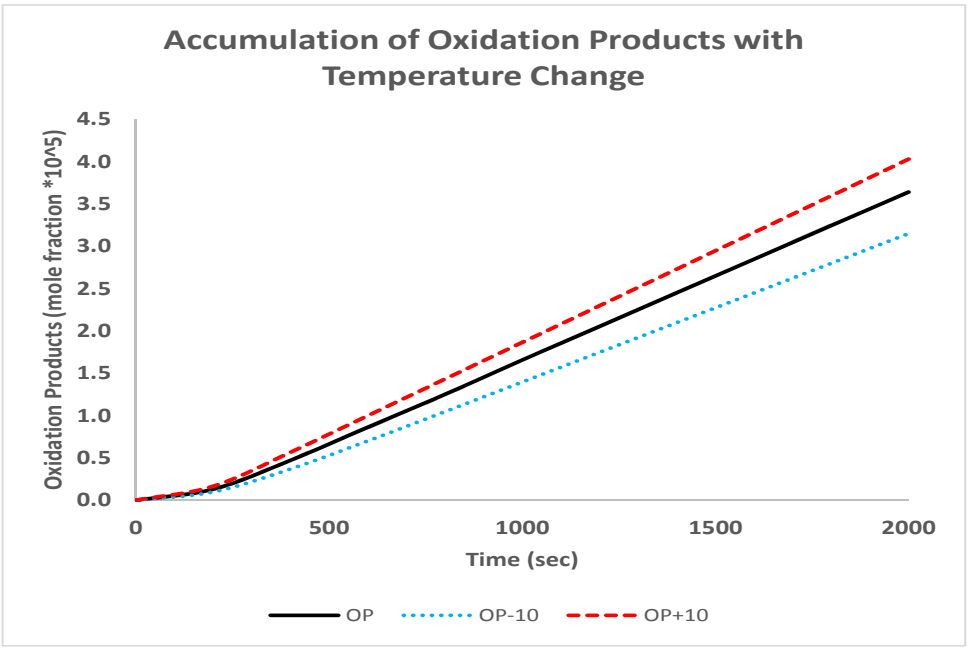

Figure 3.8: Effect of temperature change on a) CO_2 absorption and b) accumulation of oxidation products, for Run 280509, AGL Loy Yang Pilot Plant

temperature is decreased by 10^{o} when using a time period of 16 minutes. Over the same period, 13.5% less oxidation products were formed. (See Figure 3.8). When the average temperature of the column is increased by 10^{o}, absorption of CO_2 is decreased by 1.7% and the formation of oxidation products is increased by 10.5%.

Chapter 4

Degradation

4.1 Assessing Oxidative Degradation of MEA

Up to this stage the validation of this model has been based on the data produced once the model has reached a relatively steady state. This has been done in order to assess the validity of the model before using it to calculate the rate of degradation of MEA and accumulation of the oxidation products that are produced as a consequence of this degradation. To assess the rate of oxidative degradation of MEA the data needs to be analysed over a long period of time rather than at steady state. This program was run for a simulation period of 400000 seconds (111.1 hours) and the data produced by the simulation was used to calculate the kilograms of MEA lost per tonne of CO_2 produced as predicted by the model using Run 280509.

It is known that the expected value for the number of kilograms of MEA lost per tonne of CO_2 captured should be in the range 0.2 to 3.0 [33, 42, 59]. These figures were produced from laboratory experiments and one pilot plant where the feed gas was approx 5% O_2 on a dry basis. Typically the O_2 concentration in flue gas streams is 6% wet [81]. In the AGL Loy Yang PCC pilot plant, the O_2 concentration in the feed gas was in the range of 5-8% on a wet basis which, when to converted to a dry basis, is higher than that for the laboratory experimental data.

4.1.1 Degradation of MEA

Using the information from the data provided by the CSIRO PCC pilot plant at AGL Loy Yang for run 280509, 15.7 kg of CO_2 is produced per operating hour. Thus it takes 63.69 hours to collect 1 tonne of CO_2. Reading from the computer model for this run, 26.286 moles of MEA are lost in 111.1 hours which is 0.01443 kilogram of MEA lost in 1 hour. Thus 0.919 kg of MEA is lost per tonne of

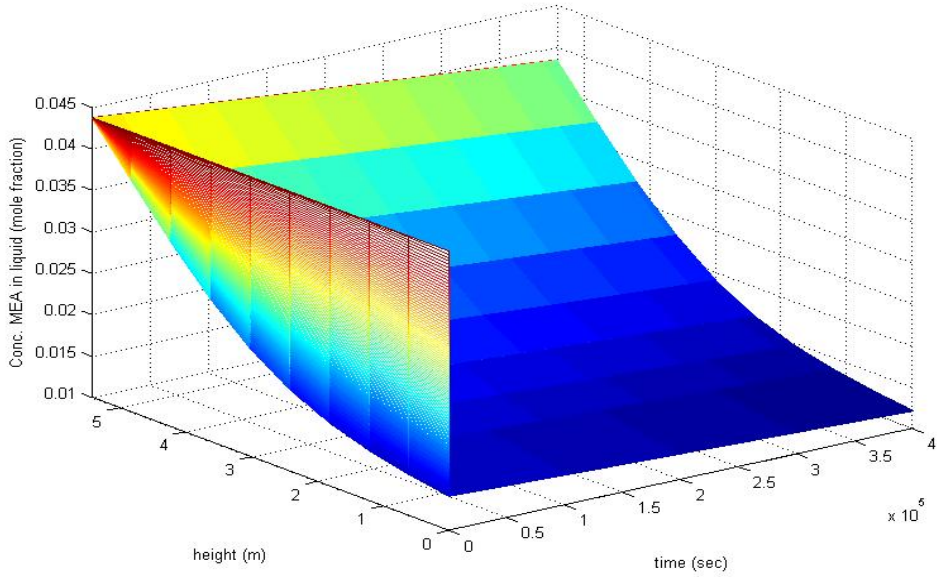

Figure 4.1: Degradation of MEA (mole fraction), Run 280509, Loy Yang Pilot Plant

CO_2 recovered which is within the range cited previously. Some of this loss is by vapourisation into the gas phase. Using the values in the computer model to quantify the vapourisation of MEA after a simulation of 111.1 hours it was found that:.

Concentration of gas leaving absorber	$= 40.06$ moles m^3
Flow rate of gas	$= 0.035$ m^3 sec^{-1}
Moles of gas per sec	$= 1.402079$
Mole fraction MEA in gas	$= 9.3303 \times 10^{-8}$
Moles of MEA in gas	$= 1.3082 \times 10^{-7}$moles sec^{-1}
Mass of MEA in gas	$= 2.87 \times 10^{-5}$kg hr^{-1}

Loss of MEA to vapourisation during the absorption of 1 tonne of CO_2 is 1.83×10^{-3} kg. According to the literature, [25], 0.08kg of MEA is lost by thermal degradation per tonne of CO_2 produced when the temperature of the stripper is 381 K.

$$\text{Total loss of MEA} = \text{loss by vapourisation} + \text{loss by oxidative degradation} + \text{loss by thermal degradation} \quad (4.1)$$

$$= 1.83 \times 10^{-3} + 0.919 + 0.08 \quad (4.2)$$

$$\text{Total loss of MEA} = 1.00083\text{kg per tonne of } CO_2 \quad (4.3)$$

This would make a total loss of MEA to the system of approximately 1.00083 kg per tonne of CO_2. Figure 4.1 shows the decreasing input concentration of MEA in the liquid over the simulated time of 111.1 hours. The mathematical model constructed in this thesis was used to quantify the accumulation of components that resulted as a consequence of oxidative degradation of MEA.

4.1.2 Accumulation of oxidation products (OP)

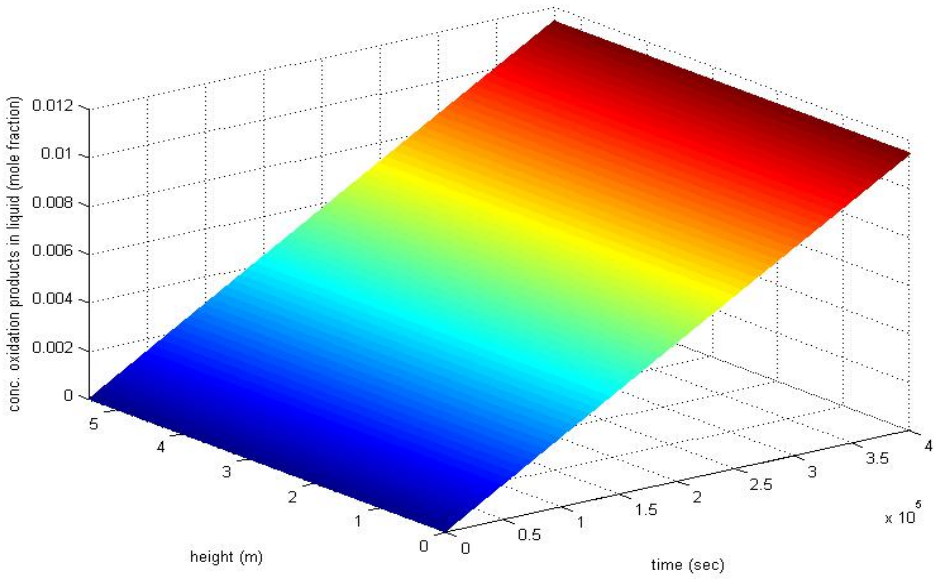

Figure 4.2: Accumulation of oxidation products (mole fraction), Run 280509, Loy Yang Pilot Plant

From the computer model, 0.0056 mole fraction MEA is lost in 111.1 hours while 0.0112 mole fraction of OP is accumulated. This reflects the increasing trend seen in Figure 4.2 which shows the accumulation of oxidation products.
Using the total number of moles in the system at time 400000 seconds (from the model), 26.286 moles MEA are lost while 52.57 moles of OP are accumulated.
If the oxidation products (OP) are assumed to be one third each of oxalic acid, formic acid and glycolic acid, then the average molecular weight is 70.70 g mol^{-1}.

$$\text{Gain OP} = \frac{52.57 \times 70.70}{1000} \times \frac{3600}{400000} \tag{4.4}$$

$$\text{Gain OP}(\text{kg hr}^{-1}) = 0.033450$$

A gain of 0.033450 kg hr^{-1} of OP is equivalent to an accumulation of 2.13 kg OP per tonne of CO_2 produced. Natural gas power plants (NGCC) operate with a much lower level of CO_2 but higher level of O_2 when compared to brown coal power plants [13]. Where the brown coal system has 12% CO_2 and 6% O_2 in the input flue gas, natural gas has 4% CO_2 and 12% O_2. Figure 4.3 compares the comparative rates of absorption of CO_2 in a NGCC and a PCCC power plant generated by the model developed in this thesis. As the input flue gas passes up the column in a PCCC plant, 68% of the CO_2 is removed whilst in the NGCC plant, 72% of CO_2 is removed. The different levels of O_2 and CO_2 in the input feed gas has minimal effect on the absorption of CO_2. However, the model predicts that the accumulation of oxidation products in a natural gas plant is 4.8 times the accumulation in a brown coal power plant over the same period of time. This is in agreement with work done by Leonard [49].

Figure 4.3 shows the rates of accumulation of oxidation products when concentrations of 4% CO_2 and 12% O_2 are included in the gaseous phase of the model. The absorbent is still MEA. This has large cost, waste and emissions implications for a natural gas plant compared to a coal plant and would suggest that an oxidation resistant absorbent should be used for the removal of CO_2 from the gaseous effluent in a NGCC plant. The input temperatures of the gas and the liquid streams to the NGCC plant were lowered by 10°K to assess the effect on the chemistry. The model predicts that the accumulation of oxidation products is reduced by 21% while the absorption of the CO_2 is only reduced by 1.2% (see Fig. 4.3b)

a)

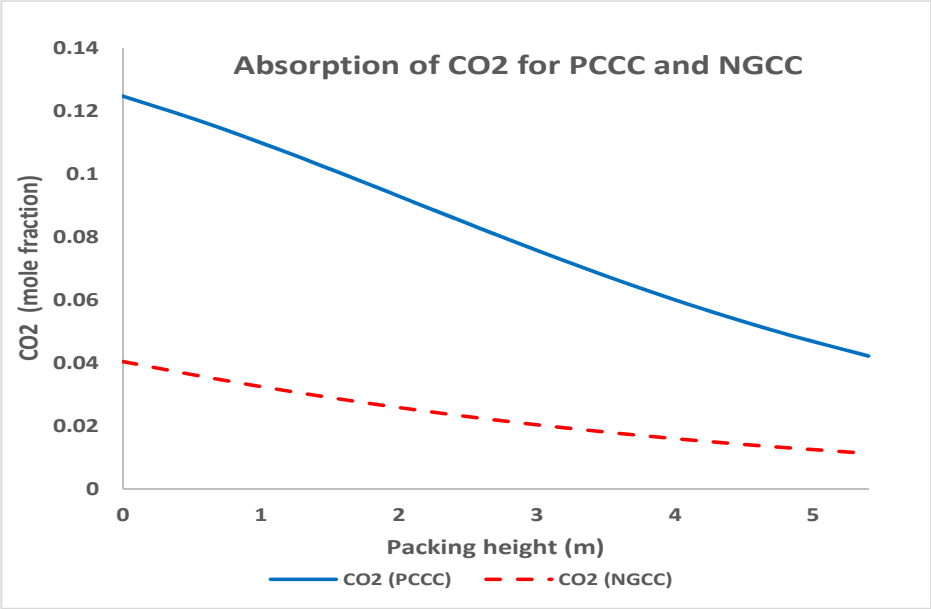

b)

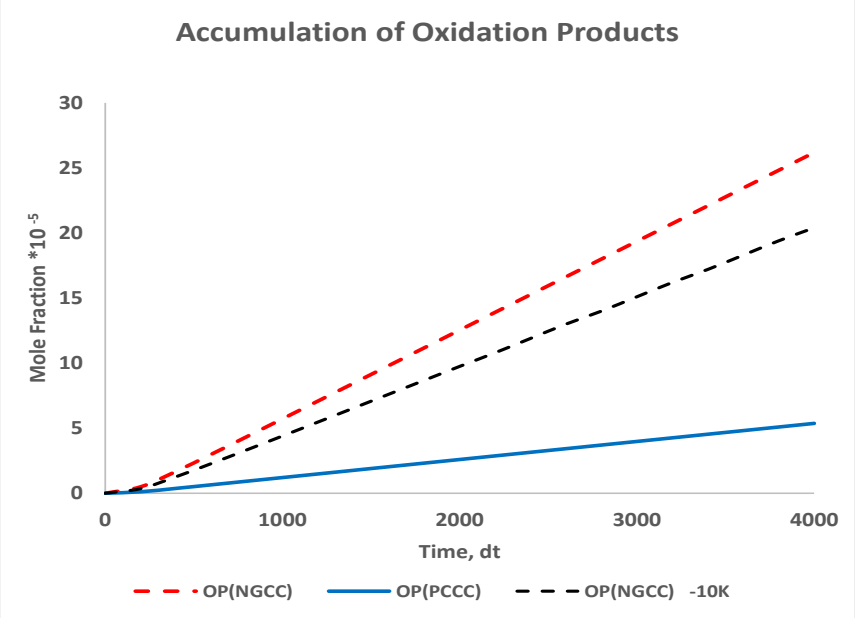

Figure 4.3: a) Absorption of CO_2 b) Accumulation of oxidation products in NGCC and PCCC power plants

Chapter 5

Conclusions

Much work has been done evaluating technologies to capture CO_2 from gaseous industrial effluent. For large-scale emitters such as coal and natural gas-fired power plants, technology using amine solvents to capture post-combustion CO_2 is the most mature CO_2 capture technology. This technology can be retrofitted to existing plants, treating the flue gas after the combustion stage. The model in this thesis is constructed from first principles and, while it is built using MEA as the absorbent to remove CO_2, it can be adjusted to cater for the removal of different industrial gases with various absorbents. The ODE's developed in the mathematical model are solved using a solver, MATLAB Ode15s. The model was found to be stable for a period of 111 hours and shows no sign of collapsing. The flux of MEA, CO_2, O_2 and H_2O across the phase interface in either direction has been included and this can be added to as required.
The loss of MEA through oxidative degradation has been quantified, a feature that is not currently available in existing commercial packages. Reaction rate kinetics have been employed to predict the accumulation of oxidation products but the accuracy of prediction is influenced by the incomplete knowledge of the precise kinetics of the dominant reactions between O_2 and MEA. When research has produced more detailed information on the products formed during this oxidation, it can be inserted easily into the model. Validation has been performed using laboratory data from CSIRO, Newcastle, and data from the CSIRO PCC pilot plant at AGL Loy Yang. It was found that 1.00083 kg of MEA was lost by vapourisation and oxidation and thermal degradation per tonne of CO_2 removed from the flue gas. This is well within the range of 0.2 to 3.0 kg of MEA predicted by the literature. The accumulation of the oxidation products as a results of oxidative degradation of MEA was found to be 2.13kg per tonne of CO_2 removed.
Gaseous effluent from natural gas power plants contains a much higher concentration of O_2 and lower concentration of CO_2 than that seen at CSIRO Newcastle or the PCC pilot plant at AGL Loy Yang. The model constructed for this thesis was

used to study the effect that this would have on the rate of build-up of oxidation products using MEA as the absorbent. It was found that MEA degrades 4.8 times faster than it does in a brown coal power plant and it would be inadvisable to use it under high O_2 conditions. A parametric study of the impact of operating conditions on oxidation showed that the accumulation of oxidation products increases as the input temperatures increase. This accumulation also increases with a high level of O_2 and low levels of CO_2 such as are found in NGCC power plants.
The key findings of this thesis are:

- quantification of the rate of oxidative degradation of MEA
- quantification of the rate of accumulation of oxidative products as a result of the degradation of MEA
- prediction of accumulation rate of oxidative products in a natural gas power plant as 4.8% greater that of a brown coal power plant
- effect of reducing the temperature of the input gas and liquid by 10°K on the rate of accumulation of oxidative products in a natural gas power plant

This work has provided CSIRO with a dynamic model that can predict oxidative degradation which the current commercial packages are unable to do.
Further model development would include:

- more investigation into the effect changing parameters has on the rate of absorption and degradation of the absorbent
- investigation of the influences on the accumulation rate of the oxidation products
- the incorporation of the other components of the absorption/desorption system, the main one being the stripper itself
- use of other absorbents, for example piperazine or a mixture of absorbents, in the model
- incorporate more detailed chemistry for the oxidation reaction between MEA and CO_2 as this becomes available

This model could and should be used for the design of industrial CO_2 capture plants to contribute to their large-scale deployment and to quantify the accumulation of oxidation products resulting from the degradation of the solvent under varying conditions.

Appendix A

A.1 Glossary

a	specific surface area of packing ($m^2 m^{-3}$)
a_w	effective interfacial area of packing per volume of packing ($m^2\ m^{-3}$)
a_{wl}	effective interfacial area of packing per volume of liquid holdup ($m^2\ m^{-3}$)
a_{wg}	effective interfacial area of packing per volume of gas holdup ($m^2\ m^{-3}$)
C	concentration (mole fraction)
C_p	heat capacities ($J\ mol^{-1}\ K^{-1}$)
c_h, c_l, c_v	packing constants specific to type of packing
D_{li}	liquid phase diffusion coefficient of i ($m^2\ s^{-1}$)
D_{gi}	vapour phase diffusion coefficient of i ($m^2\ s^{-1}$)
d_H	heat generated by reactions ($J\ mol^{-1}$)
d_h	hydraulic diameter of random packing (m)
dz	height interval (m)
E	enhancement factor
G	gas flow ($mol\ m^{-3}$)
g	gravitational constant ($m\ s^{-2}$)
H_{CO_2}	Henry's constant for carbon dioxide ($Pa\ m^3\ mol^{-1}$)
H_{O_2}	Henry's constant for oxygen ($Pa\ m^3\ mol^{-1}$)
h_l	liquid hold-up ($m^3\ m^{-3}$)
h_g	gas hold-up ($m^3\ m^{-3}$)
h_T	heat transfer coefficient ($W\ m^2\ K$)
$[i]$	concentration of component i ($mol\ m^{-3}$)
K_g	overall mass transfer coefficient ($mol\ Pa^{-1}\ m^{-2}\ s^{-1}$)
k_f	forward reaction rate ($mol\ m^{-3}\ s^{-1}$)
k_g	mass transfer coefficient in vapour phase ($mol\ Pa^{-1}\ m^{-2}\ s^{-1}$)
k_l	mass transfer coefficient in liquid phase ($m\ s^{-1}$)
k_r	reverse reaction rate (s^{-1})
L	liquid flow ($mol\ m^{-3}$)

MW	Molcular Weight
N	molar flux between phases ($mol\ m^{-2}\ s^{-1}$)
P	partial pressure in bulk vapour (Pa)
P^*	equilibrium partial pressure in bulk liquid (Pa)
P_{vp}	partial vapour pressure (Pa)
R	Universal gas constant ($m^3\ Pa\ mol^{-1}\ K^{-1}$)
Rx	reaction rate ($mol\ m^{-3}\ s^{-1}$)
r_{O_2}	rate of oxidative degradation ($mol\ m{-}3$)
T	temperature (K)
T_C	temperature in celsius ($Celsius$)
T_c	critical temperature (K)
t	time (s)
u_g	velocity of gas phase ($m\ s^{-1}$)
u_G	velocity of gas with respect to the empty column cross section ($mol\ s^{-1}$)
u_l	velocity of liquid phase ($m\ s^{-1}$)
u_L	velocity of liquid with respect to the empty column cross section ($mol\ s^{-1}$)
V	molar volume ($cm^3\ mol^{-1}$)
z	height of column (m)
ΔH_abs	heat of absorption ($J\ mol^{-1}$)
ΔH_{react}	heat of reaction ($J\ mol^{-1}$)
ΔH_{vap}	heat of vapourisation or condensation($J\ mol^{-1}$)
ϵ	void fraction of column ($m^3\ m^{-3}$)
λ	thermal conductivity of the gas ($W\ m^{-1}\ K^{-1}$
ν_{dl}	dynamic viscosity of liquid ($kg\ m^{-1}\ s^{-1}$)
ν_{kl}	kinematic viscosity of liquid ($kg\ m^{-3}$)
ν_{kg}	kinematic viscosity of gas ($kg\ m^{-3}$)
ν_{H_2O}	viscosity of H_2O cP
Ω	Lennard-Jones potential (dimensionless)
ρ	density ($kg\ m^{-3}$)
σ	collision diameter (A)
σ_l	surface tension ($kg\ m^{-2}$)

subscripts and superscripts

i	component
g	gas
l	liquid

A.2 Parameters

Parameters for Newcastle Column
RUN A

Diameter	0.15m		
Packing	16mm S/S Pall Rings		
L/G	2.734		
Pressure	130.4kPa		
Packed Ht	2.4m		
Gas Inlet conditions		Solvent Inlet conditions	
Temp	40.12^o C	Temp	39.3^o C
N_2 flow	36.28 kg/hr	Flow rate	119.99 kg/hr
CO_2O flow	5.866 kg/hr	MEA conc	0.3% wt
H_2O flow	1.742 kg/hr	H_2O conc	0.7% wt

RUN B

Diameter	0.15m		
Packing	16mm S/S Pall Rings		
L/G	4.214		
Pressure	132.6 kPa		
Packed Ht	2.4m		
Gas Inlet conditions		Solvent Inlet conditions	
Temp	36.47^o C	Temp	40.82^o C
N_2 flow	25.92 kg/hr	Flow rate	121.10 kg/hr
CO_2O flow	4.208 kg/hr	MEA conc	0.3% wt
H_2O flow	1.219 kg/hr	H_2O conc	0.7% wt

Parameters for Loy Yang Pilot plant
RUN 280509

Diameter Packing L/G	0.20m 25mm S/S Pall Rings 2.97		
Pressure Packed Ht	101.35 kPa 5.4m		
Gas Inlet conditions		Solvent Inlet conditions	
Temp N_2 flow CO_2O flow H_2O flow O_2 flow	43.3^o C 118.27 kg/hr 22.45 kg/hr 5.74 kg/hr 7.13 kg/hr	Temp Flow rate MEA conc H_2O conc	42.55^o C 153.59 kg/hr 0.26% wt 0.74% wt

RUN 061011

Diameter Packing L/G	0.20m 25mm S/S Pall Rings 6.44		
Pressure Packed Ht	102.47 kPa 5.4m		
Gas Inlet conditions		Solvent Inlet conditions	
Temp N_2 flow CO_2O flow H_2O flow O_2 flow	52.00^o C 44.94 kg/hr 14.04 kg/hr 1.42 kg/hr 6.39 kg/hr	Temp Flow rate MEA conc H_2O conc	48.54^o C 153.59 kg/hr 0.35% wt/wt 0.65% wt/wt

A.3 Physical & chemical properties

Parameter	Units	Reference
Column liquid hold-up	$m^3\ m^{-3}$	Billet and Schultes 1999
Diff. coeff. of CO_2, O_2 & H_2O in gas	$m^2\ s^{-1}$	Poling et al. 2001
Diff. coeff. of CO_2, O_2 & MEA in liquid	$m^2\ s^{-1}$	Poling et al. 2001
Diff. coeff. of MEA in gas	$m^2\ s^{-1}$	Kvamsdal 2009
Dynamic liquid viscosity	$N\ m\ s^{-2}$	Weiland et al. 1998
Heat of absorption of CO_2	$J\ mol^{-1}$	Crovetto 1990
Heat of absorption of O_2	$J\ mol^{-1}$	Dana 1925 [24]
Heat of vapourisation of H_2O	$J\ mol^{-1}$	Kvamsdal 2009
Heat of vapourisation of MEA	$J\ mol^{-1}$	MSDS Cameo Chemicals
Heat capacity for gases	$J\ mol^{-1}\ K^{-1}$	Poling et al. 2001
Heat Capacity for liquid MEA	$J\ mol^{-1}\ K^{-1}$	Maham et al. 1997
Heat Capacity for liquid H_2O	$J\ mol^{-1}\ K^{-1}$	Perry et al. 1997
Heat Capacity for liquid carbamate	$J\ mol^{-1}\ K^{-1}$	Ruzicka et al. 1993
Heat transfer coeff.	$J\ s^{-1}\ m^{-2}\ K^{-1}$	Bird et al. 2002
Henry's law constant for CO_2	$Pa\ m^3\ mol^{-1}$	Crovetto 1991
Henry's law constant of O_2	$Pa\ m^3\ mol^{-1}$	
Kinematic liquid viscosity	$m^2\ s^{-1}$	Weiland et al. 1998
Liquid surface tension	$N\ m^{-1}$	Vazquez et al. 1997
Mass transfer coeff. for gases & liquids	$m\ s^{-1}$	Billet and Schultes 1999
Reaction rates for MEA and CO_2	$k_f = m^3\ mol^{-1}\ sec^{-1}$ $k_r = s^{-1}$	Conway 2011
Reaction rate for MEA and O_2	$K = mol\ m^{-3}\ sec^{-1}$	Leonard 2014
Specific wetted area	$m^2\ m^{-3}$	Billet and Schultes 1999
Thermal conductivity of gases	$J\ s^{-1}\ m^{-1}\ K^{-1}$	Lide [52] 2006
Vapour pressure of H_2O	Pa	Perry et al. 1997
Viscosity of water	$N\ m\ s^{-2}$	Cussler 1996

A.4 Vienna MATHMOD 2015 Conference

8th Vienna International Conference on Mathematical Modelling
February 18 - 20, 2015. Vienna University of Technology, Vienna, Austria

IFAC
INTERNATIONAL FEDERATION OF AUTOMATIC CONTROL

Further Developments in Dynamic Modelling of CO_2 Capture from Flue Gas

Jillian Dickinson* Graeme Puxty**
Andrew Percy*, T. Vincent Verheyen*****

*School of Applied Sciences and Engineering, Faculty of Science,
Monash University, Australia (Tel: [redacted]
**CSIRO Energy Flagship, Newcastle, Australia [redacted]
***School of Applied and Biomedical Sciences, FederationUniversity,
Churchill, Australia [redacted]

Abstract:

Mathematical modelling of CO_2 capture from industrial flue gas by absorption into amine solutions such as monoethanolamine (MEA) has been undertaken for decades and steady state, rate-based and dynamic models have been constructed to predict the changes in the process. Recently, dynamic models have been used to predict the effect that physical operational changes have on the absorption process. As more is learnt about the chemistry of MEA and CO_2 it becomes evident that the absorption system is losing available MEA, by degradation and by vaporization into the gaseous phase. This paper describes a dynamic model of the absorber column that can be used to predict the reduction of available MEA, the loss of MEA to the atmosphere, and the build-up of heat stable salts. The proposed mathematical model consists of a system of partial differential equations to represent the change of each component with height of the column and with time. It has been validated with data from a pilot capture plant located at the brown coal fired Loy Yang power station in Australia.

Keywords: Dynamic modelling; differential equations; carbon capture; oxidative degradation; absorption; chemical industry.

1. INTRODUCTION

A world-wide concern about pollution and climate change has led to detailed investigations into how to remove unwanted components from industrial gaseous effluent. There is increasing evidence of the contribution of carbon dioxide to global warming (IPCC, 2007). This has led to the removal of acid gases (such as oxides of carbon, nitrogen and sulphur) from industrial gaseous effluent becoming a major objective for many research groups. It is thought that the release of these gases into the atmosphere is contributing to a change of the Earth's climate. Sulphur and nitrogen oxides are the cause of localised environmental problems such as acid rain but these can be managed with existing technology. Oxides of carbon, in particular carbon dioxide emissions occur in far greater amounts, are generated across the globe and are more challenging to address.

Removal of these acid gases from gaseous effluent by absorption into a solvent is an accepted and proven method that has been used in the chemical and petrochemical industries for many decades. Absorption into a solvent is being investigated for application to other industries whose flue gases contain large quantities of carbon dioxide, such as those burning fossil fuels to produce electricity (Artanto, 2012; Saimpert, 2013).

Absorption of CO_2 is carried out by counter-currently contacting a gas stream with an absorbent liquid in a packed column. Mathematical models have been developed to describe this absorption process but, to simplify the model, they have used many assumptions including that the column is operating in a steady state (Simon, 2010; Mores, 2012). These models assume that equilibrium has been reached at all points in the column which is not a true representation of the absorption column. These steady state models simulate the change of concentration and temperature over the height of the column but are not able to be used for accurate prediction of the state of the column after a prolonged period of time because these models do not incorporate slow chemical reactions (Greer 2008, Øi 2010).

Dynamic models have been designed that can predict the response within the column to changing physical operating conditions such as input gas properties (Bui, 2014, Lawal et al, 2010). These models do not assume that equilibrium has been reached at all points and are a closer representation of the real conditions. However, the current dynamic models do not include information about the transfer from one phase to the other of some of the important process components, nor the degradation of the solvent. The volatility and the oxidative degradation of the absorbent are long term time-dependent changes that are important to the efficiency of the overall system of absorption.

This paper describes a dynamic mathematical model which can predict the movement of any required component from liquid to gas and gas to liquid. It can also predict long term

changes such as the amount of liquid absorbent which is degraded by reaction with oxygen under the conditions at which the column operates. Current dynamic mathematical models do not predict this aspect of the changing chemistry within the absorber column.

The inclusion of oxidative degradation was chosen as the focus for this work as oxygen has been identified as a critical component affecting the absorption process in the flue gas. Solvent oxidation leads to the formation of degradation products some of which may be emitted to the atmosphere. It is also a major contributor to solvent cost because of the need to top up the solvent concentration. The inclusion of solvent oxidation in the model allows for optimisation of process conditions, both in terms of absorption performance as well as the minimisation of oxidative degradation. It should also be noted that given the appropriate chemical knowledge the model could also be easily extended to include other longer term processes such as thermal degradation and nitrosamine formation.

2. THE ABSORPTION PROCESS

The capture and removal of the carbon dioxide is a two stage process and consists of separate packed absorption and desorption columns. The process relies on the reversible reaction between carbon dioxide and an amine, most commonly monoethanolamine (MEA), the direction of the reaction is dependent on the operating temperature. At lower temperatures such as are found in the absorber column, the reaction (1) proceeds to the right and dissolved CO_2 forms a carbamate. When the temperature is increased in the desorber column, the reaction is reversed and the carbamate breaks down into its components, MEA and CO_2 allowing the acid gas to be collected. The overall reversible equation can be written as:

$$CO_2 + 2MEA \leftrightarrow MEACOO^- + MEAH^+ \quad (1)$$

There is some discussion as to the actual mechanism of the formation of the carbamate. It is thought to occur in two steps (Versteeg 1996),

$$CO_2 + MEA \leftrightarrow MEACOO^- + H^+ \quad (2)$$
$$H^+ + MEA \leftrightarrow MEAH^+ \quad (3)$$

with (2) being slower than (3) and is thus the rate determining step.

Within the absorption column, the flue effluent, rich in the carbon dioxide, is introduced to the bottom of the column in counter-current contact with an aqueous MEA solution. Carbon dioxide moves from the gas phase across the gas/liquid interface into the liquid phase. The packing in the column makes a larger surface area available for liquid-gas mass transfer. The CO_2 reacts immediately with the active solvent component and the heat sensitive carbamate is formed.

The gaseous effluent which is now lean in CO_2, is released into the atmosphere. The solution, rich in the carbamate, continues through the system and is pumped from the bottom of the absorber column to the top of the desorber column. The elevated temperatures in the desorber column cause the reaction to be reversed and the carbon dioxide is released. The gaseous effluent from the desorber column consists of CO_2 and water, it is dried and the pure carbon dioxide is collected for storage or for further use. The lean MEA solution is removed from the bottom of the desorber, passed through a heat exchanger to reduce its temperature before being returned to the top of the absorber and made available for further reaction with CO_2. Figure 1 is a representation of the complete absorption/desorption process which details the flow of input vapour and liquid phases but does not show external heat exchangers, condensers, etc.

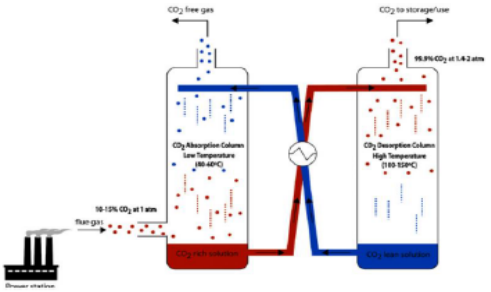

Fig 1. Simplified diagram of the absorption-desorption process. (Simon 2011)

3. STATEMENT OF THE PROBLEM

This process can be applied to the removal and capture of the carbon dioxide from the flue gases of brown coal fired power stations. There are several different types of liquid absorbents that are being trialled for the absorption of CO_2 including alkali metal hydroxides and amines. MEA is typically included as a standard reference solvent given its long history in gas processing (Pellegrini 2010).
The absorption process involves the movement of components from one phase to the other driven by the concentration differentia.

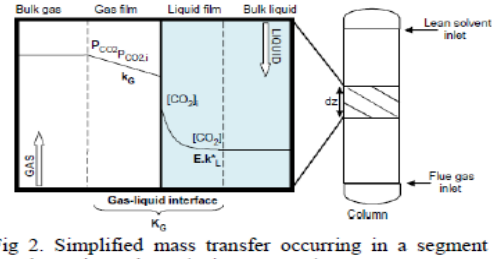

Fig 2. Simplified mass transfer occurring in a segment of absorption column (Saimpert 2012).

Figure 2 is an indicative sketch of the concentration gradient of CO_2 across the interface within a section of the absorber column.

Reactions take place in the liquid, some of which are of great importance, such as (1) and the oxidation reaction(4):

$$O_2 + MEA \rightarrow \text{oxidation products} \quad (4)$$

For many years, mathematical models have been developed for this process that have been based on a steady state in the column and considered concentrations and temperatures to be functions of only one variable, height of the column. These models did not include any reaction kinetics. This has limited their use, particularly with the increasing desire to understand the composition of the gaseous effluent and the process of degradation when using an amine solvent.

Because of the complexity of the chemistry and the size of the calculations, many assumptions have had to be made to produce a model that partially reflects reality (Gaspar 2010). These models assumed that the only component transfer across the interface was that of CO_2 and that there was no reaction between O_2 and MEA. Now that computers are capable of calculating more complex sets of equations and at a faster rate, more variables can be included in the models.

More recently dynamic mathematical models have been developed which include two variables, height and time and consequently can model some reaction kinetics. They have been used to investigate what happens to the absorption process when input factors change, such as increased flow rate of the gas, or increased operating temperature (Gaspar 2011, Saimpert 2013). These models can be used to determine the most efficient operating conditions for the absorption system but currently do not tell us about oxidative degradation of MEA nor include the true movement of components across the gas-liquid interface. The degradation of the solvent is an important aspect of the absorption process as the liquid absorbent is continually recycled throughout the column and any MEA loss results in decreased quantity of liquid sorbent available for the absorption of CO_2. Thus the MEA needs to be replaced in order to maintain effective CO_2 capture. This replacement adds to the cost of the process.

4. DEVELOPMENT OF THE DYNAMIC MODEL

This dynamic mathematical process model is a system of partial differential equations incorporating with both space and time as variables. They are used to describe the effects of operational changes on the column but more importantly, the real time degradation of MEA with oxygen. The backward and forward finite difference method has been employed to account for the height variable while the Matlab ode15 solver has been used for the numerical solution of the time variable. Using finite difference for the height variable in the partial differential equations gives us ordinary differential equations in the time variable. The model contains a differential equation for each of the components of interest in the liquid and gaseous phases, and for the temperature of each phase. The components included in the model are MEA, H_2O, $MEACOO^-$, $MEAH^+$, CO_2, O_2 in the liquid phase and H_2O, CO_2, O_2, MEA and N_2 in the gaseous phase. In the liquid phase there is also a general term for any oxidation products that occur as a result of reaction between MEA and O_2. However, there is no differential equation for nitrogen as it is not considered to be involved in any reactions. The model uses an ODE solver for speed and accuracy of calculation.

The heat transfer terms in the differential equations for temperature consider advection, convection, heats of reaction, heats of vapourisation and absorption as well as heat change due to transportation from one phase to another. The physical properties of the system such as density, viscosity, specific heat capacity are expressed in terms of concentration and temperature and thus vary depending on the conditions at the relative position and time in the column.

The model contains the following assumptions.

- Chemical reactions take place in the liquid phase only.
- Due to small liquid phase heat transfer resistance, the liquid interface temperature can be considered equal to the bulk liquid temperature.
- The absorption column is operated adiabatically.
- The gas phase was an ideal mixture.

Mass balance equations are based on the change of concentrations with time and height and the enthalpy balance is measured by the change in temperature with time and height. The equation for the mass balance in the liquid phase states that the change of concentration of a component, i, in the liquid, C_{li}, with time, t, at height, z, is equivalent to the advection of the component in the liquid flow plus the diffusion of i into or out of the liquid phase plus the rate of generation or consumption of i due to reaction. The equation for the vapour is similar but there is no reaction term.

Component mass balances for the liquid phase is:

$$\frac{\partial C_{li}}{\partial t} = v_l \frac{\partial C_{li}}{\partial z} + \frac{a_w \cdot N_i + R_i}{L} \quad (5)$$

and for the gas phase is:

$$\frac{\partial C_{gi}}{\partial t} = v_g \frac{\partial C_{gi}}{\partial z} + \frac{a_w \cdot N_i}{G} \quad (6)$$

where subscripts li and gi represents the liquid and vapour (gaseous) phase components respectively. L and G are the liquid and gas flow rates (mol s^{-1}), N_i is the molar flux between the phases (mol m^{-2} s^{-1}), and a_w is the effective interfacial area of packing per unit volume of packing (m^2 m^{-3}). v_l and v_g are the liquid and gas velocities (m s^{-1}) with the direction of the gas flow regarded as being positive and that of the liquid flow negative.

The equation for the change of liquid temperature with time and height (7) is equal to the advection of heat content of the liquid plus the horizontal flow of heat between phases due to the temperature gradient plus the heat released or absorbed when the components condense or evaporate plus the heat released or consumed by any reactions as well as a term for the change in temperature due to the transfer of components from one phase to the other. The gas phase heat balance (8)

consists of the advection term plus the horizontal heat flow due to the temperature gradient between the phases and a term for the change in temperature due to the transfer of components from one phase to the other.

Heat balance for the liquid phase is:

$$\frac{\partial T_l}{\partial t} = v_l \frac{\partial T_l}{\partial z} + \frac{h_T \cdot a_w \cdot (T_l - T_g)}{\rho_l \cdot c_{pl}} + \frac{h_T \cdot N_i \cdot \Delta H_{vap}}{\rho_l \cdot c_{pl}} + \frac{\Delta H_{react}}{\rho_l \cdot c_{pl}} + \frac{a_w \cdot N_i \cdot c_{pl} \cdot (T_l - T_g)}{\rho_l \cdot c_{pl}} \quad (7)$$

and for the gas phase is:

$$\frac{\partial T_g}{\partial t} = v_g \frac{\partial T_g}{\partial z} + \frac{h_T \cdot a_w \cdot (T_g - T_l)}{\rho_g \cdot c_{pg}} + \frac{a_w \cdot N_i \cdot c_{pg} \cdot (T_g - T_l)}{\rho_l \cdot c_{pg}}. \quad (8)$$

The densities of the liquid and the gas, ρ_l and ρ_g, (mole m^{-3}) the specific heats of the liquid and the gas, c_{pl}, and c_{pg}, (J mole^{-1} K^{-1})as well as the heat of vapourisation/condensation, ΔH_{vap}, and the heat of reaction, ΔH_{react}, are all functions of the concentration of the reactants and the temperature of the phases.

In order to track oxidative degradation, consideration needs to be given to reactions between O_2 and MEA. Due to the many possible reactions between these two compounds, it is difficult to choose one reaction that is more important than the others for oxidative degradation (Bello 2005). It has been noted by Velvestad that there are 19 reactions that could take place between O_2 and MEA depending on the conditions within the column (Velvestad 2011). Work has been done by Léonard to construct a relationship which he has proven represents the reaction rate between O_2 and MEA in the presence of either CO_2, SO_2 or both (Léonard 2014).

$$-r_{MEA} = 5.53 * 10^5 e^{-\frac{41,780}{RT}} [O_2]^{1.46} \quad (10)$$

R is the Universal Gas Constant (J mol^{-1}K^{-1}) and T is the degradation temperature (K). The value for the activation energy is given in J mol^{-1} and the pre-exponential unit is (mol L^{-1} s^{-1})(mol L^{-1})$^{-1.46}$. Since MEA is always in excess its influence on the oxidative degradation can be assumed constant.

This reaction rate has been incorporated into the dynamic model described here, which allows it to predict the amount of MEA which has been involved in the formation of degradation products but does not tell us what the degradation products are. By knowing the amount of MEA involved in oxidative degradation and the quantity vapourised to the gaseous phase under specific column conditions, it is possible to determine the loss of MEA over time during the absorption process. This dynamic model can be used to determine which operating conditions result in good absorption of the CO_2 but with minimal loss of available MEA.

Figures 3-5 are examples of the graphs that are generated by the model. As the absorption column is assumed to initially contain liquid absorbent but no gaseous effluent, the first results for the height of the column for each graph are constant. The flue exhaust gas is admitted to the bottom of the absorber column at time zero and the concentration changes rapidly until the gas reaches the full height of the column. This results in the initial concentration conditions for the height of the model for each of the following graphs showing as a straight line.

Figure 3 is a graph of the change in concentration of carbon dioxide in the vapour phase which shows the concentration of the acid gas reducing as the vapour progresses up the height of the column. It also indicates that the system is stabilising as time progresses. This trend agrees with the mass transfer of CO_2 into the liquid phase.

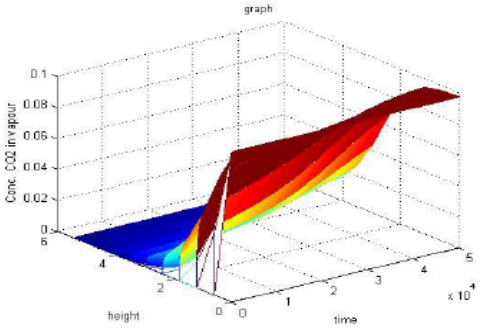

Fig 3. Change of concentration of CO_2 in vapour. (Height in metres and time in secs)

Figure 4 is the graph of the change of concentration of MEA in the liquid phase. The liquid phase is fed into the column from the top.

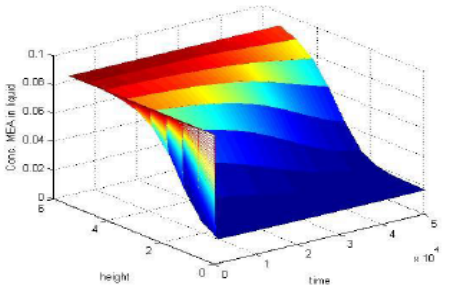

Fig 4. Change of concentration of MEA in the liquid phase. (Height in metres and time in secs)

The decreasing concentration of the absorbent MEA is due to the formation of the carbamate compound, oxidation products and evaporation of MEA into the vapour phase thus reducing the mole fraction of MEA in the liquid available for further reaction with other components. The resulting MEA solution is passed through the desorber column before being returned to the top of the absorber column. The mole fraction of the MEA in the inlet liquid slowly decreases due to accumulation of oxidation products from the oxidative degradation of MEA and also its volatility.

Figure 5 is a graph of the temperature of the liquid in the absorber column and shows the change in temperature with height mainly as a result of the exothermic reactions in the liquid and subsequent heat exchange. It also shows the bulge in the temperature towards the top of the column which is reflective of the operating conditions as seen by other modellers (Saimpert 2013, Greer, 2008, Jayarathna, 2013).

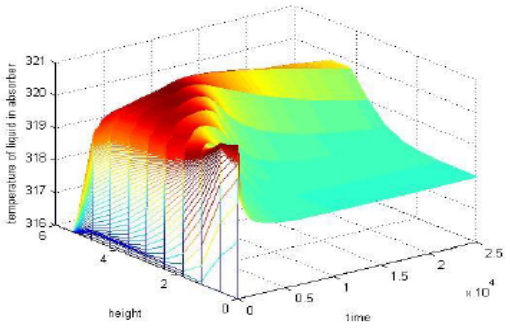

Fig 5 Graph of temperature of the liquid in the absorber column. (Height in metres and time in secs)

Figures 6 and 7 compare the model results with the available pilot plant experimental results for the change of carbon dioxide and the temperature of the liquid and gas phases of the absorption column. This pilot plant only has input and output data, hence the lack of data points for the comparison.

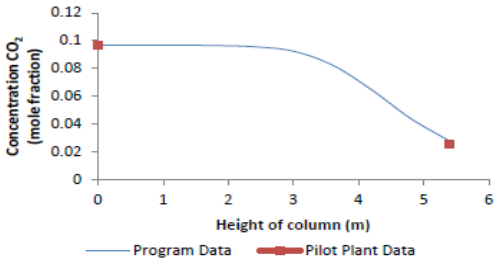

Fig 6 Carbon Dioxide in the vapour

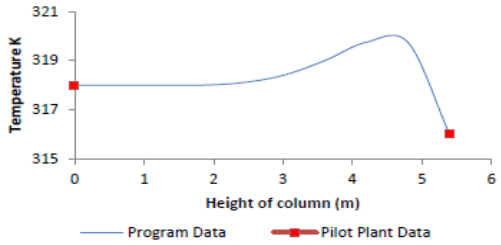

Fig 7 Temperature of the liquid and gas phases

The model's predicted concentration and temperature values 13.8 hours after start-up were compared with the experimental data obtained from the pilot plant during stable operation. The blue line represents the data points generated by the model and the red points are experimental results from the pilot plant.

The model also predicted that the mole fraction of MEA in the input liquid should decrease from 0.0902 to 0.0899, over the 13.8 hour period, due to the formation of oxidation products. There is no experimental data to verify this finding.

5. SUMMARY

This dynamic mathematical model has been built primarily to determine the loss of MEA by oxidative degradation during the process of absorbing CO_2. It can also be used to predict the changes of absorption rates and efficiencies within the absorber column when operational changes, such as flow rate, concentrations or temperatures are made. The dynamic model can be used to represent any gas separation process which uses a liquid absorbent as the input parameters can be easily changed to reflect the properties of other detailed absorption processes. It has been validated using real data from a pilot plant which has been retrofitted to an existing brown coal fired power station in Australia where the boiler flue gases can be fed into the pilot plant for assessment. Work is continuing on this model to incorporate the desorber column into the cycle.

6. REFERENCES

Artanto, Y. et al. (2012). A preliminary evaluation of post-combustion CO_2 capture performance in a pilot plant test using monoethanolamine at a lignite-fuelled power station in Australia. in *Fourth International Conference of Clean Coal Technologies for our Future (CCT2009).* 2009. Dresden, Germany: IEA Clean Coal Centre.

Bello, A., and Idem, R., (2005). Pathways for the formation of products of the oxidative degradation of CO_2-loaded concentrated aqueous monoethanolamine solutions during CO_2 absorption from flue gases *Ind.Eng.Chem.Res.* 44. 945-969

Bui, M., et al., (2014). Dynamic modelling and optimisation of flexible operation in post-combustion CO_2 capture

plants—A review. *Computers & Chemical Engineering* 2014. 61(0): 245-265.

Gaspar, J. and Cormos, A., (2011). Dynamic modelling and validation of absorber and desorber columns for post combustion CO_2 capture. *Computers and Chemical Engineering*. 35. 2044-2052.

Greer, T., (2008) Modeling and simulation of post combustion CO_2 capture. *Master Thesis - Telmark University College*.

Intergovernmental Panel on Climate Change (IPCC). (2007). *4th Assessments Report, Climate change*. www.ipcc.ch

Jayarathna, S., Lie, B., & Melaaen, M., (2013). Dynamic modelling of the absorber of a post-combustion CO_2 capture plant: Modelling and simulations. *Computers and Chemical Engineering*. 53. 178-189.

Lawal, A., Wang, M., Stephenson, P., Koumpouras, G., & Yeung, H., (2010). Dynamic Modelling and analysis of post-combustion CO_2 chemical absorption process for coal-fired power plant. *Fuel*. 89, 2791-2801.

Léonard, G., Toye, D., & Heyen, G., (2014). Experimental study and kinetic model of monoethanolamine oxidative and thermal degradation for post-combustion CO_2 capture. *International Journal of Greenhouse Gas Control*. 30. 171-178.

Mores, P., Scenna, N. and Mussati, S. (2012). A rate based model of a packed column for CO_2 absorption using aqueous monoethanolamine solution. *International Journal of Greenhouse Gas Control*. 6. 21-36.

Øi, L., (2010). CO_2 removal by absorption: challenges in modelling. *Mathematical and computer modelling of dynamic systems*. 16(6) 511-533.

Pellegrini, G., Strube, R. and Manfrida, G., (2010). Comparative study of chemical absorbents in post combustion CO_2 capture. *Energy*. 35. 851-857.

Saimpert, M., Puxty, G., Qureshi,S., Wardhaugh, L. and Cousins, A. (2013) A new rate based absorber and desorber modelling tool. *Chemical engineering science*. 96. 10-25.

Simon, L. L., Elias, Y., Puxty, G., Artanto, Y and Hungerbuhler, K. (2011). Rate based modelling and validation of a carbon dioxide pilot plant absorption column operating on monoethanolamine. *Chemical Engineering Research and Design*. 89 (9), 1684-1692.

Supap, T., Idem, R., Tontiwachwuthikul, P. and Saiwan, C. (2009). Kinetics of sulphur dioxide- and oxygen-induced degradation of aqueous monoethanolamine solution during CO_2 absorption from power plant flue gas streams. *International Journal of Greenhouse Gas Control,* 3, 133-142.

Velvestad, S., Eide-Haugmo, I., da Silva, E. and Svendsen, H., (2011). Degradation of MEA; a theoretical study. *Energy Procedia*. 4 1608-1615.

Versteeg, G.F., Van Dick, L.A.J., and Van Swaaij, W.P.M., (1996). On the kinetics between CO_2 and alkanolamines both in aqueous and non-aqueous solutions. An overview. *Chemical Engineering Communications*. 144, 113-158.

Bibliography

[1] A. Aboudheir, P. Tontiwachwuthikul, A. Chakma, and R. Idem. Kinetics of the reactive absorption of carbon dioxide in high CO_2-loaded, concentrated aqueous monoethanolamine solutions. *Chemical Engineering Science*, 46:5195–5210, 2003.

[2] Mohammad R.M. Abu-Zahra, John P.M. Niederer, Paul H.M. Feron, and Geert F. Versteeg. CO_2 capture from power plants: Part ii. a parametric study of the economical performance based on mono-ethanolamine. *International Journal of Greenhouse Gas Control*, 1:135 – 142, 2007.

[3] I. Alatiqi, M. Sabri, W. Bouhamra, and E. Alper. Steady-state rate-based modelling for CO_2/amine absorption-desorption systems. *Gas Separation and Purification*, 8:3–11, 1994.

[4] C. E. Alie, L. Backham, E. Croidset, and P. L. Douglas. Simulation of CO_2 capture using MEA scrubbing: a flowsheet decomposition method. *Energy Conversion and Management*, 46:475–487, 2005.

[5] Y. Artanto, J. Jansen, P. Pearson, T. Do, A. Cottrell, and E. Meuleman. Performance of MEA and amine-blends in the CSIRO PCC pilot plant at Loy Yang Power in Australia. *Fuel*, 101:264–275, 2012.

[6] U.E. Aruno, H.F. Svensden, K.A. Hoff, and O. Juliussen. Solvent selection for carbon dioxide absorption. *Energy Procedia*, 1:1051–1057, 2009.

[7] S. Bedell. Oxidative degradation mechanisms for amines in flue gas capture. *Energy Procedia*, 1:771–778, 2009.

[8] A. Bello and R. Idem. Pathways for the formation of products of the oxidative degradation of CO_2-loaded concentrated aqueous monoethanolamine solutions during CO_2 absorption from flue gases. *Ind. Eng. Chem. Res.*, 44:945–969, 2005.

[9] C. Biliyok, A. Lawal, M. Wang, and F. Seibert. Dynamic modelling, validation and analysis of post-combustion chemical absorption CO_2 capture plant. *International Journal of Greenhouse Gas Control*, 9:428 – 445, 2012.

[10] R. Billet and M. Schultes. Prediction of mass transfer columns with dumped and arranged packings. *Trans IChemE*, 77:498–504, September 1999.

[11] D. Billingsley and A. Chirachavala. Numerical solution of nonequilibrium multicomponent mass transfer operations. *AIChE Journal*, 27:968–974, November 1981.

[12] R. Bird, W. Stewart, and E.N. Lightfoot. *Transport Phenomena*. John Wiley and Sons, 2002.

[13] J. Black. Cost and performance baseline for fossil energy plants volume 1: Bituminous coal and natural gas to electricity, revision 2. Technical report, Department of Energy, National Energy Technology Laboratory, 2010.

[14] G. Blauwhoff, P. Versteeg, and W. Van Swaaij. A study on the reaction between CO_2 and alkanolamines in aqueous solutions. *Chemical Engineering Science*, 39:207–225, 1984.

[15] M. Bui, I. Gunawan, T.M. Verheyen, P. Feron, E. Meuleman, and S. Adeloju. Dynamic modelling and optimisation of flexible operation in post-combustion CO_2 capture plants a review. *Computers & Chemical Engineering*, 61:245 – 265, 2014.

[16] X. Chen. *Carbon Dioxide Thermodynamics, Kinetics and Mass Transfer in Aqueous Piperazine Derivatives and other Amines*. PhD thesis, University of Texas at Austin, 2011.

[17] F.A. Chowdhury and H. Okabe. Synthesis and selection of hindered new amine absorbents for CO_2 capture. *Energy Procedia*, 4:201–208, 2011.

[18] W. Conway, Y. Beyad, G. Richner, G. Puxty, and P. Feron. Rapid CO_2 absorption into aqueous benzylamine (BZA) solutions and its formulations with monoethanolamine, and 2-amino-2-methyl-1-propanol (AMP) as components for post combustion capture processes. *Chemical Engineering Journal*, 264:954–961, 2015.

[19] A. Cormos, J. Gaspar, and A. Padurean. Modeling and simulation of carbon dioxide absorption in monoethanolamine in packed absorption columns. *Studia Universitatis Babes-Bolyai*, 3:37–48, 2009.

[20] A. Cottrell, J. McGregor, J. Jansen, Y. Artanto, N. Dave, S. Morgan, P. Pearson, M. Attalla, L Wardhaugh, H. Yu, A Allport, and P. Feron. Post-combustion capture R & D and pilot plant operation in australia. *Energy Procedia 1*, pages 1003–1010, 2009.

[21] R. Crovetto. Evaluation of solubility data of the system CO_2-H_2O from 273 K to the critical point of water. *J. Phys. Chem. Ref. Data.*, 20:575–589, 1990.

[22] E. Cussler. *Diffusion. Mass Transfer in Fluid Systems.* Cambridge University Press, 2009.

[23] E. Da Silva and H. Svendsen. Computational chemistry study of reactions, equilibrium and kinetics of chemical CO_2 absorption. *Greenhouse Gas Control*, 1:151–157, 2007.

[24] L. Dana. The latent heat of vapourization of liquid Oxygen-Nitrogen mixtures. *Proceedings of the American Academy of Arts and Sciences*, 60:241–267, 1925.

[25] J. Davis and G. T. Rochelle. Thermal degradation of monoethanolamine at stripper conditions. *Energy Procedia*, 1:327–333, 2009.

[26] Y. Elias. Carbon-dioxide (CO_2) absorption pilot plant column modeling and validation. Master's thesis, Safety and Environmental Technology group, 2008.

[27] N. Enaasen, H. Knuutila, H. Kvamsdal, and M. Hillestad. Dynamic model validation of the post-combustion CO_2 absorption process. *International Journal of Greenhouse Gas Control*, 41:127–141, 2015.

[28] R. Ewing and H. Wang. A summary of numerical methods for time-dependent advection-dominated parrtial differential equations. *Journal of Computational and Applied Mathematics*, 128:423–445, 2001.

[29] L. Faramarzi, G. Kontogeorgis, M. Michelsen, K. Thomsen, and E. Stenby. Absorber model for CO_2 capture by monoethanolamine. *Industrial & Engineering Chemistry Research*, 49:3751–3759, 2010.

[30] L. Formaggia, F. Saleri, and A. Veneziana. *Solving Numerical PDEs: Problems, Applications Exercises.* Springer - Vertag Italia, 2012.

[31] J. Gabrielsen. *CO_2 Capture from Coal Fire Power Plants.* PhD thesis, technical University of Denmark, 2007.

[32] J. Gaspar and A. Cormos. Dynamic modeling and validation of absorber and desorber columns for post-combustion CO_2 capture. *Computers and Chemical Engineering*, 35:2044–2052, 2011.

[33] G. Goff and G. Rochelle. Monoethanolamine degradation: O_2 mass transfer effects under CO_2 capture conditions. *Ind. Eng. Chem. Res.*, 43:6400–6408, 2004.

[34] T. Greer. Modeling and simulation of post combustion CO_2 capturing. Master's thesis, Telemark University College, 2008.

[35] T. Greer, S. Jayarathna, M. Alic, M. Melaaen, and B. Lie. Dynamic model for removal of carbon dioxide from a post combustion process with monoethanolamine. In *MATHMOD 09 Vienna*, 2009.

[36] N. Harun, P. Douglas, L. Ricardez-Sandoval, and E. Croiset. Dynamic simulation of MEA absorption processes for CO_2 capture from fossil fuel power plant. *Energy Procedia*, 4:1478–1485, 2011.

[37] W. Hunsdorfer and J.G. Verwer. *Numerical Solution of Time-Dependent Advection-Diffusion-Reaction Equations*. Springer, 2003.

[38] S. Jayarathna, B. Lie, and M. Melaaen. Simulations of the dynamic operation of the absorber of a CO_2 capture plant. In *International Conference on Environmental Pollution and Remediation*, 2011.

[39] S. Jayarathna, B. Lie, and M. Melaaen. Amine based CO_2 capture plant: Dynamic modeling and simulations. *International Journal of Greenhouse Gas Control*, 14:282 – 290, 2013.

[40] S. Jayarathna, B. Lie, and M. Melaaen. Dynamic modelling of the absorber of a post-combustion CO_2 capture plant: Modelling and simulations. *Computers and Chemical Engineering*, 53:178 – 189, 2013.

[41] E. Kenig, R. Schneider, and A. Gorak. Rigorous dynamic modelling of complex reactive absorption processes. *Chemical Engineering Science*, 54:5195–5203, 1999.

[42] J. Knudsen, J. Jensen, P. Vilhelmsen, and O. Biede. Experience with CO_2 capture from coal flue gas in pilot-scale: Testing of different amine solvents. *Energy Procedia*, 1:783–790, 2009.

[43] A.L. Kohl and R.B. Neilsen. *Gas Purification*. Gulf Publishing, Houston, 5th edition, 1997.

[44] L. Kucka, I. Muller, E. Kenig, and A. Gorak. On the modelling and simulation of sour gas absorption by aqueous amine solutions. *Chemical Engineering Science*, 58:3571–3578, 2003.

[45] H. Kvamsdal, J. P. Jakobsen, and K. Hoff. Dynamic modeling and simulation of a CO_2 absorber column for post-combustion CO_2 capture. *Chemical Engineering and Processing*, 48:135–144, 2009.

[46] H.M. Kvamsdal and G.T. Rochelle. Effects of the temperature bulge in CO_2 absorption from flue gas by aqueous monoethanolamine. *Indust. Eng. Chem. Res.*, 47:867–875, 2008.

[47] A. Lawal, A. Wang, P. Stephenson, G. Koumpouras, and H. Yeung. Dynamic modeling and analysis of post-combustion CO_2 chemical absorption process for coal-fired power plants. *Fuel*, 89:2791–2801, 2010.

[48] A. Lawal, A. Wang, P. Stephenson, and H. Yeung. Dynamic modeling of CO_2 absorption for post combustion capture in coal-fired power plants. *Fuel*, 88:2455–2462, 2009.

[49] G. Leonard, Toye D., and G. Heyen. Experimental study and kinetic model of monoethanolamine oxidative and thermal degradation for post-combustion CO_2 capture. *International Journal of Greenhouse Gas Control*, 30:171–178, 2014.

[50] D. Lepaumier, A. Grimstvedt, K. Vernstad, K. Zahlsen, and H. Svendsen. Degradation of MMEA at absorber and stripper conditions. *Chemical Engineering Science*, 66:3491–3498, 2011.

[51] D. Lepaumier, D. Picq, and P.L. Carrette. New amines for CO_2 capture. II. oxidative degradation mechanisms. *Industrial Engineering and Chemical Research*, 48:9068–9075, 2009.

[52] D.R. Lide. *CRC Handbook of Chemistry and Physics*. CRC Press, Boca Raton, Fl, 87 edition, 2006.

[53] N. MacDowell, N.J. Samsatli, and N. Shah. Dynamic modelling and analysis of an amine-based post-combustion CO_2 capture absorption column. *International Journal of Greenhouse Gas Control*, 12:247–258, 2013.

[54] N. McCann, D. Phan, X. Wang, W. Conway, R. Burns, M. Attalla, G. Puxty, and M. Maeder. Kinetics and mechanism of carbamate formation from CO_2 (aq), carbonate species, and monoethanolamine in aqueous solution. *J. Phys. Chem. A*, 113:5022–5029, 2009.

[55] J. McLees. Vapor-liquid equilibrium of monoethanolamine/piperazine/water at 35-70^o C. Master's thesis, University of Texas, 2006.

[56] J. Mertens, H. Lepaumier, D. Desagher, and M. Thielens. Understanding ethanolamine (MEA) and ammonia emissions from amine based post combustion carbon capture: Lessons learned from field tests. *International Journal of Greenhouse Gas Control*, 13:72 – 77, 2013.

[57] P. Mores, N. Scenna, and et al. Post-combustion CO_2 capture process: Equilibrium stage mathematical model of the chemical absorption of CO_2 into monoethanolamine (MEA) aqueous solution. *Chemical Engineering Research and Design*, 89:1587–1599, 2011.

[58] P. Mores, N. Scenna, and et al. A rate based model of a packed column for CO_2 absorption using aqueous monoethanolamine solution. *International Journal of Greenhouse Gas Control*, 6:21–36, 2012.

[59] P. Moser, S. Schmidt, G. Sieder, H. Garcia, and T. Stoffregen. Performance of MEA in a long-term test at the post-combustion capture pilot plant in Niederaussem. *International Journal of Greenhouse Gas Control*, 5:620–627, 2011.

[60] L.E. Oi. CO_2 removal by absorption: challenges in modelling. *Mathematical and Computer Modelling of Dynamical Systems*, 16:511–533, 2010.

[61] K. Onda, E. Sada, T. Kobayashi, and M. Fujine. Gas absorption accompanied by complex chemical reactions - I. Reversible chemical reactions. *Chemical Engineering Science*, 25:753–760, 1970.

[62] R. Pachauri and A. (Eds) Reisinger. 4th assessment report - climate change. Technical report, Intergovernmental Panel on Climate Change, 2007.

[63] J. Pandya. Adiabatic gas absorption and stripping with chemical reaction in packed towers. *Chemical Engineering Communications*, 19:343–361, 1983.

[64] D. Pinto, T. Brodtkorb, S. Vevelstad, H. Knuutila, and H. Svendsen. Modeling of oxidative MEA degradation. *Energy Procedia*, 63:940 – 950, 2014.

[65] B. Poling, J. Prausnitz, and J. O'Connell. *The Properties of Liquids and Gases*. McGraw-Hill, fifth edition, 1967.

[66] G. Puxty and R. Rowland. Carbon dioxide postcombustion capture: A novel screening study of the carbon dioxide absorption performance of 76 amines. *Environmental Science and Technology*, 43:6427–6433, 2009.

[67] T.R Rettich, R. Battino, and E. Wilhelm. Solubility of gases in liquids. 22. High-precision determination of Henry's law constants of oxygen in liquid water. *J. Chemical Thermodynamics*, 32:1145–1156, 2000.

[68] A. J. Reynolds, T. V. Verheyen, S. B. Adeloju, E. Meuleman, and P. Feron. Towards commercial scale postcombustion capture of CO_2 with monoethanolamine solvent: Key considerations for solvent management and environmental impacts. *Environmental Science & Technology*, 46:3643–3654, 2012.

[69] G. Richner, G. Puxty, A. Carnal, W. Conway, M. Maeder, and P. Pearson. Thermokinetic properties and performance evaluation of benzylamine-based solvents for CO_2 capture. *Chemical Engineering Journal*, 264:230–240, 2015.

[70] P. Rooney, M. DuPart, and T. Bacon. Oxygen's role in alkanolamine degradation. *Hydrocarbon Processing*, pages 109–113, July 1998.

[71] M. Saimpert, G. Puxty, S. Qureshi, L. Wardhaugh, and A. Cousins. A new rate based absorber and desorber modelling tool. *Chemical Engineering Science*, 96:10–25, 2013.

[72] R. Schneider and A. Gorak. Model optimization for the dynamic simulation of reactive absorption processes. *Chemical Engineering Technology*, 24:979–989, 2001.

[73] R. Schneider, E. Kenig, and A. Gorak. Dynamic modelling of reactive absorption with the Maxwell-Stefan approach. *Trans IChemE*, 77:635–638, 1999.

[74] R. Schneider, F. Sander, and A. Gorak. Dynamic simulation of industrial reactive absorption processes. *Chemical Engineering & Processing*, 42:955–964, 2003.

[75] J. Seader. The rate-based approach for modeling staged separation. *Chemical Engineering Progress*, 85:41–49, 1989.

[76] A. Sexton and G. Rochelle. Reaction products from the oxidative degradation of monoethanolamine. *Ind. Eng. Chem. Res*, 50:667–673, 2011.

[77] L. Simon, Y. Elias, G. Puxty, Y. Artanto, and K. Hungerbuhler. Rate based modeling and validation of a carbon-dioxide pilot plant absorption column operating on monoethanolamine. *Chemical Engineering Research & Design*, 89:1684–1692, 2011.

[78] B. Strazisar, R. Anderson, and C. White. Degradation of MEA used in CO_2 capture from flue gas of a coal-fired electric power generating station. *Energy and Fuels*, pages 1–80, 2003.

[79] P. Suess and L. Spiegel. Hold-up of Mellapak structured packings. *Chemical Engineering and Processing*, pages 119–124, 1992.

[80] T. Supap, R. Idem, P. Tontiwachwuthikul, and C. Saiwan. Analysis of monoethanolamine and its oxidative degradation products during CO_2 absorption from flue gases: A comparative study of GC-MS, HPLC-RID, and CE-DAD analytical techniques and possible optimum combinations. *Ind. Eng. Chem. Res.*, 45:2437–2451, 2006.

[81] T. Supap, R. Idem, P. Tontiwachwuthikul, and C. Saiwan. Kinetics of sulfur dioxide- and oxygen-induced degradation of aqueous monoethanolamine solution during CO_2 absorption from power plant flue gas streams. *International Journal of Greenhouse Gas Control*, 3:133–142, 2009.

[82] J. Svensden and D. Eimer. Case studies of CO_2 capture columns based on fundamental modeling. *Energy Procedia*, 4:1419–1426, 2011.

[83] E. Tadmor. A review of numerical methods for nonlinear partial differential equations. *Bulletin of the American Mathematical Society*, pages 1–48, July 2012.

[84] F. Tobiesen. *Modelling and Experimental study of Carbon Dioxide Absorption and Desorption*. PhD thesis, Norwegian University of Science and Technology, 2007.

[85] F. Tobiesen and H. Svendsen. Experimental validation of a rigorous absorber model for CO_2 post-combustion capture. *AIChE Journal*, 53:846–865, 2007.

[86] I. Uyanga and R. Idem. Studies of SO_2- and O_2-induced degradation of aqueous MEA during CO_2 capture from power plant flue gas streams. *Ind. Eng. Chem. Res.*, 46:2558–2566, 2007.

[87] G. Versteeg, L. Van Dijck, and W. Van Swaaij. On the kinetics between CO_2 and alkanolamines both in aqueous and non-aqueous solutions: An overview. *Chem. Eng. Comm.*, 144:113–158, 1996.

[88] S.J. Vevelstad, I. Eide-Haugmo, E.F. da Silva, and H.F. Svendsen. Degradation of MEA: A theoretical study. *Energy Procedia*, 31:1608–1615, March 1984.

[89] A.K. Voice and G.T. Rochelle. Oxidation of amines at absorber conditions for CO_2 capture from flue gas. *Energy Procedia*, 4:171–178, 2011.

[90] M. Wang, A. Lawal, P. Stephenson, J. Sidders, and C. Ramshaw. Post-combustion CO_2 capture with chemical absorption: A state-of-the-art review. *Chemical Engineering Research and Design*, 89:1609–1324, 2011.

[91] R. Weiland, J. Dingman, D. Cronin, and G. Browning. Density and viscosity of some partially carbonated aqueous alkanolamine solutions and their blends. *J. Chem. Eng. Data*, 43:378–382, 1998.

[92] Y. Zhang, H. Chen, C. Chen, J. Plaza, R. Dugas, and G. Rochelle. Rate-based process modeling study of CO_2 capture with aqueous monoethanolamine solution. *Ind. Eng. Chem. Res.*, 48:9233–9246, 2009.